Systemic Risk of Commodity Traders*

Zeno Adams†, Thorsten Glück‡

August 9, 2023

Abstract

We examine the disruptions to global commodity flows following the bankruptcy of a commodity trading firm. The physical commodity network is operated by a handful of large traders that are responsible for the timely delivery of raw materials and inputs to industrial production. We propose a model that simulates the resilience and response time of the network following a shock. Our results suggest that a number of commodity traders carry significant systemic risk. The forced removal of a trader from the network has considerable implications for the prices and availability of physical commodities over a period of 6 to 12 months.

Keywords: Systemic Risk; International Trade; Commodity Trading Firms

JEL Classifications: Q40, Q41, Q43

*We would like to thank Bernd Brommundt, Alexis Derviz, Steffen Meyer, Jon Olaf Olaussen, Are Oust, Daria Zeko and various commodity traders at BP and Glencore for valuable comments and suggestions. This work is supported by SNF no. 100018_178903. Donglin He and Maria Kartsakli provided research assistance.

†University of St.Gallen, School of Finance, Unterer Graben 21, CH-9000 St. Gallen, Switzerland; Tel.: +41 71 224 7014; E-mail address: zeno.adams@unisg.ch.

‡Corresponding author. Wiesbaden Business School, Hochschule RheinMain, DE-65183 Wiesbaden, Germany; Tel.: +49 (0) 611 94953145; E-mail address: thorsten.glueck@hs-rm.de.

1 Introduction

Commodity trading firms operate the global flow of natural resources. They are responsible for the timely delivery of primary inputs to industrial production. In this paper, we examine the question whether the failure of a commodity trading firm has systemic implications for the real economy. Systemic risk is a key research topic in financial economics that is typically associated with financial institutions. A large and mature literature has proposed a number of empirical risk measures and theoretical models which explain the economic transmission channels of systemic risk for financial firms.[1] For commodity trading firms, the systemic relevance is not obvious as these firms do not hold each other's assets on their balance sheet and do not create financial links during their operations. In contrast to financial institutions, there is thus no systemic risk within the network of commodity traders. Instead, we argue that the systemic relevance of commodity trading firms is due to their vital function as providers of raw materials to manufacturing and industrial production. Natural resource deposits are concentrated within a few countries and need to be transported by ship to the regions in which they are consumed. Commodity traders are specialist firms that manage the logistical operations of those heavy, bulky, and sometimes toxic commodities. We show that the forced removal of a commodity trader from this network of physical flows can lead to a disruption of the supply chain in the buyer regions that is reflected in lower local supply and higher prices. The dynamics of this negative supply shock persist until other traders gradually replace the missing trade routes left by the failed company.

The theoretical foundation for our paper is provided in Acemoglu et al. (2012) who study the intersectoral input-output linkages in the real economy. The key insight is the fact that when one sector acts as a supplier to chains of downstream sectors, idiosyncratic shocks to the supplier can generate cascading effects that propagate to the entire economy.[2]

[1] This literature is well summarized in the overview article in Engle (2018) and more recently in Jackson and Pernoud (2021). Two prominent papers that contributed significantly to the literature and which are worth mentioning here are Adrian and Brunnermeier (2016) and Acharya et al. (2017).

[2] The traditional argument is that in a large and diversified economy with n producers, aggregate output volatility $\propto 1/\sqrt{n}$. Acemoglu et al. (2012) show that under cascading effects, this might not be the case due to first- and higher order interconnections. In particular, volatility might not vanish even if $n \to \infty$.

We illustrate this mechanism for the crude oil sector in Figure 1: a commodity trader has a trading relationship with an importing region by supplying the economy of that region with natural resources such as crude oil. Crude oil is currently the number one primary energy source in the world (see, e.g., Ritchie et al., 2022) and is refined into different energy products such as road fuels, liquefied petroleum gas, and heating oil that are used in various sectors of the economy including transportation, cooking, and heating. Whether the trader occupies a central position for the buyer economy depends on how the traded goods are further processed. Inoue and Todo (2022) denote this the "upstreamness" and compare the importance of different imported products for Japan. They show that commodities such as petroleum, coal, lumber, and plastics take a central position for the economy whereas for instance transportation equipment are semi-final products that are assembled domestically. Commodity supply shocks are therefore estimated to be of larger relevance than similar shocks for other imported products. Acemoglu et al. (2012) show that in this type of setting, a disruption of the trade link that is initially idiosyncratic in nature will have systemic economy-wide effects. Hence, commodity traders are systemically relevant even for large economies if they provide raw materials that are of crucial importance for the economy's central input producers.

Because of the systemic risk, we suggest to draw the attention to the possible consequences of a default of one or more of these traders. As a first step in this direction, we propose a model which allows us to simulate the dynamics of global commodity flows and prices within an adjustment period following a trader's default. We present a systemic risk ranking of commodity traders based on the simulated impact of trader default on a global as well as regional scale. Our model is based on the following economic mechanism: the default of a commodity trader causes some regions to have short-run flows that are smaller than their long-run counterparts. Local supply shortages increase commodity prices in the affected regions which in turn generate an incentive for the remaining traders to subsequently fill the gap left by the defaulted trader. Over time, equilibrium is restored as supply shortages are reduced and prices and quantities converge to their long-run values.

In order to keep our model manageable, we introduce three simplifying assumptions: First, we strictly distinguish between commodity seller and buyer regions with traders tak-

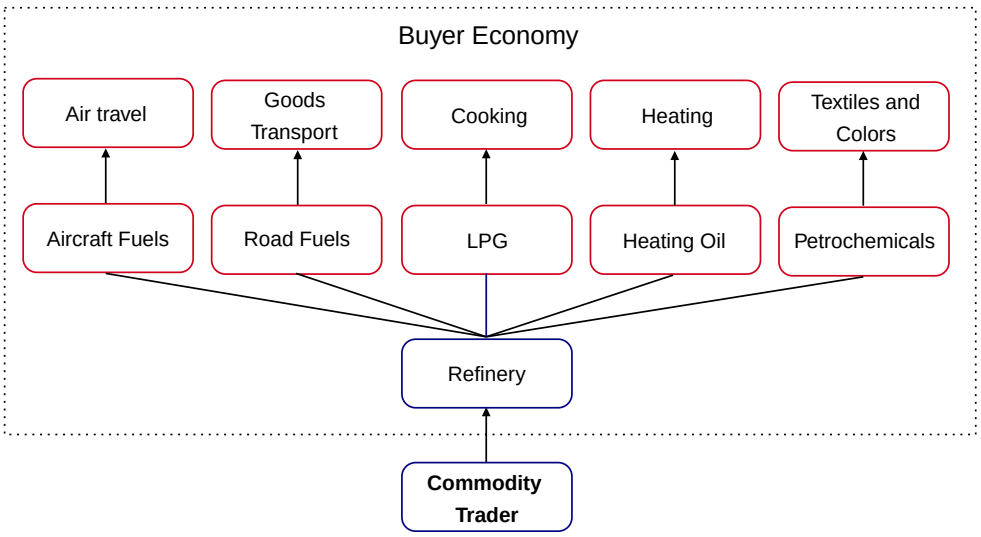

Figure 1: Systemic Spillovers from Commodity Trader Default

This figure illustrates how commodity trading firms occupy a central position in the economy's production network. Since oil is used as an input in a number of industries, the failure of the commodity trader generates a supply shock that propagates through a significant part of the real economy.

ing the role of the intermediary. There are thus no seller regions which simultaneously act as buyer regions and vice versa. Second, we assume a long-run equilibrium commodity flow matrix which determines the quantities sold from each seller to each buyer. In particular, the default of a commodity trading firm initiates a response from the remaining traders who will compensate for the local supply disruption without re-optimizing the long-term flows that are determined by this matrix. Finally, prices are the product of a global price component, a regional supply shortage margin and an additional multiplier accounting for the distance between buyer and seller region. There are hence no trader specific price components which might result from specialized knowledge or scale economies.

This basic framework of price and quantity adjustments offers three main advantages. First, our model requires the calibration of only two parameters. One parameter captures the elasticity of prices to changes in supply, the other determines the speed of the adjustment to the long-run commodity flow matrix. For the calibration of both parameters, we can resort to existing work on commodity price shocks (see Kilian, 2014). Second,

the adjustment mechanism is sufficiently general to hold for different types of commodities. Differences across commodities are reflected in their price elasticities and adjustment parameters. Third, in principle, we can easily incorporate trends in protectionism, deglobalisation, and other forms of effective reorganization in global trade patterns (Goldberg and Reed, 2020; Foti et al., 2013). Within our model, such changes would be reflected by defining an appropriate shift in the long-run flow matrix. For instance, the recent changes in international flows of energy commodities such as oil and gas as a consequence of the sanctions following the Russian invasion of Ukraine in 2022, can be modeled by shifting outflows from one seller region to another.[3]

We substantiate our model with data on 155,435 individual physical transactions operated by a total of 1,637 commodity trading firms. Based on annual data of seaborne oil trade from 2007 to 2018, we construct the long-run world oil flow matrix between 15 world trading zones. For model calibration, we utilize the flexible oil market VAR developed and applied in Baumeister and Peersman (2013a,b). We show that 10 commodity traders manage 43% of the global physical trade in crude oil and refined energy products, making physical trading a highly concentrated business. Using our model to simulate the failure of a commodity trading firm, we quantify the disruptions in trading flows and the resulting price impacts on exposed importing regions. The top 10 most systemically important energy firms include Unipec, Shell, BP, and Vitol. Our estimates suggest that the failure of one of these firms can lead to local supply disruptions of up to 16 million barrels per quarter and a short-term doubling in local oil prices. Given the focus of policy makers on energy security of households and the competitiveness of energy intensive industries, these effects are economically large. In this regard, our findings also contribute to the rich literature on oil supply shocks by providing a new perspective on the possible sources of these shocks. Finally, we also provide a new perspective on systemic risk in general, which, thus far, has been dominated by the analysis of financial institutions.

The remainder of this paper is organized as follows. Section 2 provides an overview of the scant literature on the topic and discusses commodity trading firms. We propose a

[3]Our model could also be used to simulate production shocks in macroeconomic models for aggregate output (e.g. Acemoglu et al., 2012; Gabaix, 2011). Shifts in the long-run matrix and the relationship between commodity supply shocks and aggregate output, however, is beyond the scope of this paper.

network model of physical commodity flows in section 3. The data on physical commodity transaction is detailed in section 4. The empirical results of our simulations are examined in section 5. Section 6 concludes.

2 Related Literature

Our paper is located at the intersection of the literature on physical trade and the work on systemic risk. Bernard and Moxnes (2018) provide an overview of the literature on physical trade which is centered around the network relationship between individual firms. In the terminology of the trade literature, the model we propose in this paper is a dynamic bipartite macro model: we explicitly model the time paths of prices and physical flows, buyer and seller regions only trade with each other but not among themselves, and we focus on aggregate regional flows rather than on individual firms. Although this strand of research improves our understanding of why firms trade and how the nodes of exporting and importing firms match, the network edges are taken for granted: the operation of physical flows is assumed to work flawlessly. We aim to challenge this view by examining the consequences of commodity trader default.

The trading of commodity futures and its impact on commodity markets has been extensively analyzed in the academic economics literature over the past decade (see Kang et al., 2023). However, almost no attention has been paid to the market players that are eventually responsible for the physical commodity flows. In one of the few publications on this topic, Baines and Hager (2021) provide two explanations for this phenomenon. On the one hand, the majority of commodity trading firms are privately-owned. Detailed data on the physical and financial trading activities is therefore rare. Examples for such companies in private ownership are Vitol and Cargill, major players in the energy and agricultural commodity market with an annual revenue of 225bn and 113.5bn US$ in 2019, respectively (see Baines and Hager, 2021). Data availability is even more problematic in case of the many small and largely unknown trading companies (see Eggert et al., 2017). On the other hand, the analysis is complicated by the fact that there is often no clear-cut border between traditional commodity trading, i.e. connecting commodity sellers and buyers, and upstream activities such as mining or oil drilling. A prominent example is publicly held

Glencore, after Vitol one of the biggest trading companies with an annual revenue of 256 bn US$ in 2022.[4] Glencore is nowadays heavily involved in mining activities and can be regarded as an industrial conglomerate rather than a pure trading company (Baines and Hager, 2021; Gilbert, 2021). In this paper, we examine the most traded and most produced commodity, i.e. crude oil, with major players being traditional trading companies as well as multinational oil and gas companies such as Vitol and Shell, respectively. However, there are also a number of other commodities for which trading is highly concentrated among a few large companies. This includes the market for cocoa analyzed by Oomes et al. (2016). Here, the four largest commodity traders, Olam, Cargill, Barry Callebaut, and Armajaro, have a market share of roughly 50% .

Our paper is also related to the literature on supply chain disruptions. Three noteworthy papers are Barrot and Sauvagnat (2016), Carvalho et al. (2020) and Inoue and Todo (2022). These authors study the propagation of outside economic shocks through the supply network and the extent to which economic activity is eventually reduced. Barrot and Sauvagnat (2016) examine the impact of natural disasters such as blizzards, earthquakes, floods, and hurricanes in the United States while Carvalho et al. (2020) explore the great East Japan earthquake in 2011. Inoue and Todo (2022) examine a very detailed data set of 4 million supply chain relationships for Japan and show the extent to which industries are affected by the disruption. However, the source of the disruption is unspecified and related to events such as the Covid-19 pandemic. In the empirical part below, we argue that the default of a large commodity trader can generate shocks that are comparable in economic size.

Finally, we note that our paper is closely connected to Foti et al. (2013) who examine the integrity of the global trading network by developing a model for network dynamics and simulating different types of shocks. Perhaps somewhat surprising, our paper is to a lesser extend connected to the literature on commodity trading networks, e.g. Fair et al. (2017), Wei et al. (2022) and Liu et al. (2020). These studies focus on metrics of empirical networks and not, as we do here, on the possible sources of short shocks or long-run changes to the trading network.

[4] see Statista.com

3 Model

3.1 Trading Network

We consider an economy with K regions and N traders. The number of units of a commodity sold by a seller at region R_j to a buyer at Region R_i via trader T_n at time t is denoted by $X_{ijn,t}$. To keep the trading relationships tractable, we make the following

Assumption 1 *For any region R_j and any time t there exists at least one i, n combination such that either $X_{ijn,t} > 0$ or $X_{jin,t} > 0$. If $X_{ijn,t} > 0$ then $X_{jin,t} = 0$ for all i, n. If $X_{jin,t} > 0$ then $X_{ijn,t} = 0$ for all i, n. Furthermore, $X_{jjn,t} = 0$.*

We thus abstract from regions without any trading. At each region, there are either sellers or buyers but not both simultaneously. This assumption simplifies the analysis considerably and is broadly consistent with our empirical analysis of the data on global trade flows in energy commodities which we present in section 4. For instance, the regions Middle East, North Africa, and West Africa are mainly exporters of oil and refined products whereas Europe, China, and South Asia are large importing regions for oil products. In general, certain countries or regions can be primarily regarded as sellers or buyers of a specific type of commodity. Finally, we also abstract from any trading within regions.

We consider an aggregation by traders which can be further consolidated to obtain inflows by region. We first aggregate over N traders: total commodity flows from R_j to R_i at time t are

$$X_{ij,t} = \sum_{n=1}^{N} X_{ijn,t}. \tag{1}$$

Note that, on the one hand, if there exists a j with $X_{ij,t} > 0$ then $X_{ji,t} = 0$ for all i. On the other hand, for any i with $X_{ji,t} = 0$, there exists at least one j with $X_{ij,t} > 0$. From Equation (1) we can aggregate a second time across all K regions to obtain consolidated inflows:

$$X_{i,t} = \sum_{j=1}^{K} X_{ij,t}. \tag{2}$$

For any region R_i, we get either $X_{i,t} > 0$ or $X_{i,t} = 0$. We call a region R_i with positive inflows, i.e. $X_{i,t} > 0$, a buyer region. Otherwise, the region is called seller region.

In the event of a bankruptcy of a commodity trader, supply shortages increase commodity prices resulting in higher import costs. For our analysis, we thus need to consider both, commodity flows and commodity prices. Let therefore $P_{ij,t}$ be the time t price for one unit of the commodity which has to be payed at a buyer region R_i if imported from a seller region R_j. We define this price as

$$P_{ij,t} = GD_{ij}M_{i,t}. \tag{3}$$

Parameter $G > 0$ measures a representative global commodity price. This price would be paid on a centralized exchange for a global oil benchmark such as the NYMEX WTI front-month futures contract. $D_{ij} > 1$ is a time invariant but region specific cost multiplier and accounts for the transportation costs of shipping commodities from R_j to R_i. $M_{i,t} \geq 1$ is a region specific margin multiplier that reflects regional supply shortages.[5] In equilibrium, $M_{i,t} = 1$. Note that $P_{ij,t}$ is identical for all traders, i.e. we abstract from trader specific pricing. We also do not further elaborate how $P_{ij,t}$, the income of selling one unit of the commodity, is allocated between traders and sellers.

The model setup can be interpreted as a directed network with nodes representing the regions and edges representing the trading relationships. There are two perspectives on this trading network: if the edges point from the seller to the buyer nodes, then we obtain the network of physical commodity flows and the strength of the edges are given by $X_{ij,t}$. If the edges point from the buyer to the seller nodes, we obtain the network of financial flows. In this case, the strength of the edges are given by

$$C_{ij,t} = P_{ij,t}X_{ij,t}. \tag{4}$$

Export revenues for the seller constitute import costs for the buyer so that $C_{ij,t}$ has a dual interpretation: $C_{ij,t}$ are (i) region R_j's revenues from trading with R_i and (ii) R_i's cost of all imports from region R_j. This network interpretation is illustrated in Figure 2.

[5] In case of an oversupply, we would expect $0 < M < 1$. However, we focus on trader bankruptcies which always result in a supply shortage.

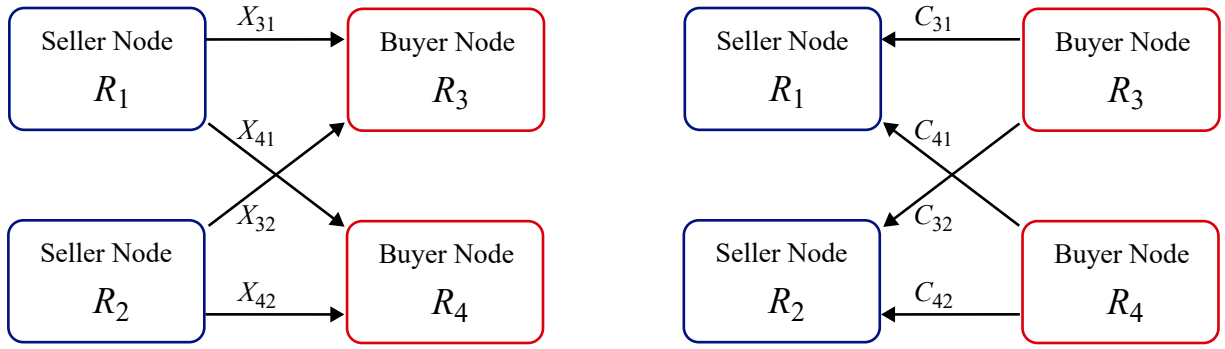

(A) Physical flows

(B) Payments

Figure 2: Illustration of a Commodity Trading Network with Two Seller- and Two Buyer Nodes

The edges in panel (A) represent physical flows X. The edges in panel (B) represent financial payments $C = PX$.

3.2 Trading Dynamics

We distinguish between long-run equilibrium and short-run adjustment dynamics. Again, to keep the model tractable, we make following simplifying

Assumption 2 *For any two regions R_i and R_j there exists a long-run commodity flow $\overline{X}_{ij} \geq 0$. The actual flows may never exceed this long-run flow, i.e. $X_{ij,t} \leq \overline{X}_{ij}$ for all t.*

In the long-run, we thus assume a fixed trading relationship with fixed flows $\overline{X}$. In addition, abstracting from short-run seller region capacities above $\overline{X}$ assures that there are no changes in long-run flows. This will become more clear in section 3.2.2 where we define the short-run adjustment process. Assumption 2 is also in line with real world capacity constraints. Commodity supply is very inelastic in the short run and many producers have little additional output capacity. For instance, the U.S. Energy Information Administration estimates that the world surplus production capacity in the period 1973 to 2021 averaged 4.4 million barrels a day.[6] The majority of this capacity is generated for strategic purposes by OPEC member countries. The non-strategic surplus production capacity was only about 500,000 barrels a day. But even the total capacity of 4.4 million barrels a day are relatively small and comparable to half of daily U.S. shale oil production in 2021.

[6] see U.S. Energy Information Administration.

The structure of our model can then be outlined as follows: The long-run inflows to buyer region R_i are $\overline{X}_i = \sum_{j=1}^{K} \overline{X}_{ij}$. These inflows balance supply and demand at R_i. Balanced supply and demand, in turn, implies a margin multiplier $M_{i,t} = 1$ and hence long-run prices and financial flows

$$\overline{P}_{ij} = GD_{ij}, \tag{5}$$

$$\overline{C}_{ij} = GD_{ij}\overline{X}_{ij}. \tag{6}$$

In the short run, we allow prices and flows to deviate from their long-run counterparts. Let therefore t_b denote the time of a trader's bankruptcy such that $X_{i,t_b} < \overline{X}_i$ for at least one buyer region R_i. The adjustment dynamics that follow the bankruptcy are driven by a fundamental economic mechanism: due to a supply shortage at some buyer region R_i, margin multiplier $M_{i,t} > 1$ such that $P_{ij,t} > \overline{P}_{ij}$. This price, in turn, sets an incentive for the remaining traders to fill the void left by the bankrupt trader. As the supply shortage is subsequently reduced, the import price approaches its long-run value and the margin multiplier $M_{i,t}$ returns to its equilibrium state in which further adjustments to flows are no longer profitable for traders. The following three properties summarize this mechanism:

(*i*) If $X_{i,t} < \overline{X}_i$ then $P_{ij,t} > \overline{P}_{ij}$ for all j,

(*ii*) If $P_{ij,t} > \overline{P}_{ij}$ for at least one j with $X_{ij,t} < \overline{X}_{ij}$, then $X_{i,t+1} > X_{i,t}$,

(*iii*) If $X_{i,t+1} > X_{i,t}$ then $P_{ij,t+1} < P_{ij,t}$ for all j.

Below, we further specify the long-run and shock time t_b trading quantities $\overline{X}_{ij}$ and X_{ij,t_b} followed by a definition of the post-shock adjustment process for quantities and prices according to the above outlined mechanism.

3.2.1 Long-run Quantities and Trader Bankruptcy

Let's assume trader T_{n_1} declares bankruptcy at t_b. We model this scenario by setting commodity flow $X_{ijn_1,t_b} = 0$ for all i, j combinations. In principle, a region with only one supplier may then experience $X_{i,t_b} = 0$. However, this special case would generate an infinite margin in our model which we rule out by the following

Assumption 3 *If a trader declares bankruptcy in t_b, then $0 < X_{i,t_b} \leq \overline{X}_i$ for all and $X_{i,t_b} < \overline{X}_i$ for at least one buyer region R_i.*

Empirically, our data shows that all regions have several suppliers. Assumption 3 is hence not particularly restrictive. Because $\overline{X}_i$ is fixed in the long run, the remaining traders $T_{n_2} \ldots, T_{n_N}$ have to subsequently fill the void left by the bankrupt trader within the post-shock period. As a result of the adjustment process outlined in the next section, for each buyer region R_i with $X_{i,t_b} < \overline{X}_i$ there is thus at least one trader $T_{n^*} \in \{T_{n_2} \ldots, T_{n_N}\}$ and one seller region R_j with $X_{ijn^*,t} > X_{ijn^*,t_b}$ for all $t > t_b + 1$.

3.2.2 Post-Shock Adjustment Process

The adjustments process is comprised of two interrelated components. The first component concerns the margin multiplier at buyer region R_i as a function of supply shortages. For some $\phi > 0$, we define

$$M_{i,t} = (\Delta X_{i,t})^{-\phi} \tag{7}$$

where $\Delta X_{i,t} = X_{i,t}/\overline{X}_i$ is the time t supply relative to long-run supply $\overline{X}_i$. In equilibrium, relative supply $\Delta X = 1$ and thus $M = 1$. If supply is below demand then $\Delta X < 1$ which implies $M > 1$. The lower the relative supply the higher the margin multiplier. Although $\Delta X = 0$ is ruled out by Assumption 3, we note that M can be arbitrarily large. However, another, possibly more realistic definition would unnecessarily complicate the model and obscure the basic economic mechanisms. Furthermore, in our application to the commodity trading data, we observe in most cases relative supply $\Delta X \geq 0.8$, i.e. the supply shortage caused by a trader's bankruptcy does not exceed 20%. We discuss this issue in more detail in section 3.3.

Once converted to logs, the economic interpretation of Equation (7) is straightforward: let $m_{i,t}$ and $\Delta x_{i,t}$ be the log values of $M_{i,t}$ and $\Delta X_{i,t}$, respectively. Equation (7) is then equivalent to

$$m_{i,t} = -\phi \Delta x_{i,t} \tag{8}$$

which shows that parameter ϕ is the price elasticity of supply: a supply reduction of 1% increases prices by ϕ%.[7]

[7]Equation (5) together with Equation (3) yields $M_{i,t} = P_{ij,t}/\overline{P}_{ij}$ and thus $m_{i,t} = \log(P_{ij,t}) - \log(\overline{P}_{ij})$.

The second component of the adjustment process concerns the magnitude by which the supply shortage is reduced. If $X_{ij,t} < \overline{X}_{ij}$ then $P_{ij,t} > \overline{P}_{ij}$, which sets an incentive for the remaining traders to build up additional transportation capacities between R_j and R_i. We model this mechanism by defining

$$\Delta X_{ij,t+1} = \Delta X_{ij,t} + \kappa_{i,t}(1 - \Delta X_{ij,t}) \tag{9}$$

where, similar as above, $\Delta X_{ij,t} = X_{ij,t}/\overline{X}_{ij}$ is the seller region R_j specific relative supply at buyer region R_i and $0 < \kappa_{i,t} < 1$ is a time and buyer region specific capacity multiplier. Equation (9) states that the R_j specific part of the time t supply shortage, given by $1 - \Delta X_{ij,t}$, is reduced by $\kappa_{i,t}$ percent between t and $t+1$. Although one could propose a number of other economically reasonable definitions for $\kappa_{i,t}$, we suggest to define for some $\psi > 0$:

$$\kappa_{i,t} = \frac{\left(M_{i,t}^{\psi} - 1\right) \Delta X_{i,t}}{1 - \Delta X_{i,t}} \tag{10}$$

which ensures that the long-run trading relationship between regions is restored after a trader's bankruptcy as shown by following

Proposition 1 *Let $0 < \psi\phi < 1$. If R_i is a buyer port with $X_{i,t_b} < \overline{X}_i$, then for any time $t \geq t_b$, the capacity multiplier satisfies $0 < \kappa_{i,t} < 1$ and the time $t+1$ relative supply is $\Delta X_{i,t+1} = \Delta X_{i,t}^{(1-\phi\psi)}$. In particular, $\Delta X_{i,t} \to 1$ and $\kappa_{i,t} \to \phi\psi$ as $(t - t_b) \to \infty$. If region R_j is a supplier for R_i with $X_{ij,t_b} < \overline{X}_{ij}$, then $\Delta X_{ij,t} \to 1$ as $(t - t_b) \to \infty$.*

The proof is provided in Appendix A.1. This definition of $\kappa_{i,t}$ has the virtue of establishing a useful and economically reasonable relationship between relative supply and margin. The higher the supply shortage the higher the margin (see Equation 7) and the increase in relative supply, i.e. the reduction of the supply shortage. A reduction of the supply shortage, in turn, implies a decrease of the margin. The adjustment process thus depicts the basic economic mechanism outlined at the beginning of this section.

We also note that, on the one hand, the relative supply increases between t and $t+1$ by approximately $\psi m_{i,t}$ percent.[8] On the other hand, we demonstrate in Appendix A.2 that for any practical purpose, κ will be virtually constant and is well approximated by is limit $\phi\psi$. The supply shortage thus decreases between t and $t+1$ by approximately $\phi\psi$ percent.

[8] To see this, rewrite $\Delta X_{i,t+1} = \Delta X_{i,t} M_{i,t}^{\psi}$. Taking logs yields $\Delta x_{i,t+1} - \Delta x_{i,t} = \psi m_{i,t}$.

3.3 Calibration for Energy Commodities

Due to our model's simplicity, we only have to determine two parameters: ϕ, which measures the price elasticity of a supply shock, and ψ, which governs the speed with which the remaining traders can accommodate a local supply shortage. To obtain realistic values, we resort to the econometric literature on the impact of oil supply shocks on macroeconomic variables. The research on this topic is usually conducted using Vector Autoregressions (VARs). In this paper, we follow Baumeister and Peersman (2013a,b) and consider a VAR with time-varying parameters and stochastic volatility for quarterly measures of global oil production, U.S. Crude Oil import prices, and world industrial production, respectively.[9] We use this model to generate a large sample of oil supply shock induced impulse response functions (IRFs) at different hypothetical states of the economy. Our choice for ϕ and ψ is then based on estimators obtained from these IRFs.

To estimate ϕ, we use the cross-section of oil supply and oil price responses after a simulated oil supply shock. Regarding ψ, we note that by Proposition 1:

$$\Delta x_{i,t} = \Delta x_{i,t_b} \left(1 - \tilde{\kappa}\right)^{(t-t_b)} \tag{11}$$

$$m_{i,t} = m_{i,t_b} \left(1 - \tilde{\kappa}\right)^{(t-t_b)} \tag{12}$$

where $\tilde{\kappa} = \phi\psi$ is, as noted above, the approximate decrease of the supply shortage in percent. Decay rate $\tilde{\kappa}$ is thus obtained by utilizing the univariate time-series of oil supply and oil prices responses for a reasonably large forecast horizon. Given estimators $\hat{\phi}$ and $\hat{\tilde{\kappa}}$, an estimator for model parameter ψ is then simply obtained via $\hat{\psi} = \hat{\tilde{\kappa}}/\hat{\phi}$. Further details regarding the VAR, the construction of IRFs and the estimation of ϕ and ψ from these IRFs can be found in Appendix B.

According to our estimations, a reasonable value for the price elasticity ϕ would be around 3, i.e. at some buyer region R_i, a decrease in the oil supply by 1% increases oil prices by approximately 3% within the same quarter. The estimators for $\tilde{\kappa}$, in turn, suggests that the decrease of the supply shortage ranges between 30% to 90% per quarter.[10] Based on these results, we define the three scenarios shown in Table 1. These scenarios are

[9] Examples of other VAR-based approaches are, among others, Lütkepohl and Netšunajev (2014), Kilian (2009), Kilian and Murphy (2014) and Blanchard and Riggi (2013).

[10] For details, see Table B1 and Table B2 in Appendix B.

motivated by the notion that the failure of a large commodity trader will likely occur in — and further contribute to — a volatile economic environment. The ability of the remaining traders to close the trade gap of the bankrupt firm will depend on their financial liquidity as well as their risk appetite for acquisition or expansion of their operations.

	Parameter ϕ: Price Elasticity of Supply		
	1.5	3.0	4.5
Parameter ψ: Speed of Output Response			
0.07	-	-	Pessimistic Scenario
0.20	-	Base Scenario	-
0.60	Optimistic Scenario	-	-

Table 1: Price Elasticity and Economic Environment
A combination of ϕ and ψ determines three possible scenarios for the size and length of an adjustment process following a commodity supply shock.

In the first scenario, we set the optimistic values $\phi = 1.5$ and $\psi = 0.6$, i.e. a moderate impact of the supply shortage on prices and, because this parameterization corresponds to $\tilde{\kappa} = 0.9$, a fast adjustment to long-run supply and prices. In the second scenario, we use $\phi = 3.0$ and $\psi = 0.2$ which implies $\tilde{\kappa} = 0.6$. This scenario serves as the base scenario and implies that the majority of the deviations from equilibirum are adjusted within two months. A recent real-world example that is in line with the baseline estimate of $\tilde{\kappa} = 0.6$ are the oil export sanctions imposed on Russia after the Ukraine invasion in 2022 which required time-intensive and costly rerouting of previously established trade links. Instead of shipping oil from the Russian ports at Primorsk or Ust Luga to Hamburg and Rotterdam within 2 weeks, oil exports are being rerouted to China which requires a round-trip voyage of 4 months.[11] Finally, in the third scenario we use the pessimistic values $\phi = 4.5$ and $\psi = 0.07$, i.e. a high impact of the supply shortage on prices and a slow adjustment

[11] A recent article in Forbes describes how this rerouting requires different types of vessels suitable for long-distance transports. Instead of the smaller Aframax tankers that carry 600,000 barrels, very Large Crude Carriers (VLCCs) that can carry 2 million barrels are needed. The shortage in vessels of this type can further prolong the shipping time which is in line with our fairly low empirical estimates.

process. In this scenario, we implicitly set $\tilde{\kappa} = 0.315$.

It should be noted that these relatively high values for ϕ correspond to a high sensitivity of the margin multiplier with respect to the supply shortage $1-\Delta X$. However, as we outline in detail in section 4.2, in most cases a trader's bankruptcy results in a shortage below 20%. Hence, $M < 1.4$ in case of the optimistic-, $M < 2.0$ in case of the base- and $M < 2.8$ in case of the pessimistic scenario (see Figure C2).[12]

As an illustration, Figure 3 shows the adjustment processes of oil supply and the oil prices for all three scenarios. In this example, the supply drops by 1% at $t = 1$. This supply shock triggers an increase of oil prices by about 1.5% in the optimistic scenario, 3.1% in the base scenario and 4.6% in the pessimistic scenario. In the optimistic scenario, oil supply and oil price correspond to their long-run values at $t = 4$, i.e. three quarters after the shock. In the pessimistic scenario, it takes 7 quarters for a full adjustment.

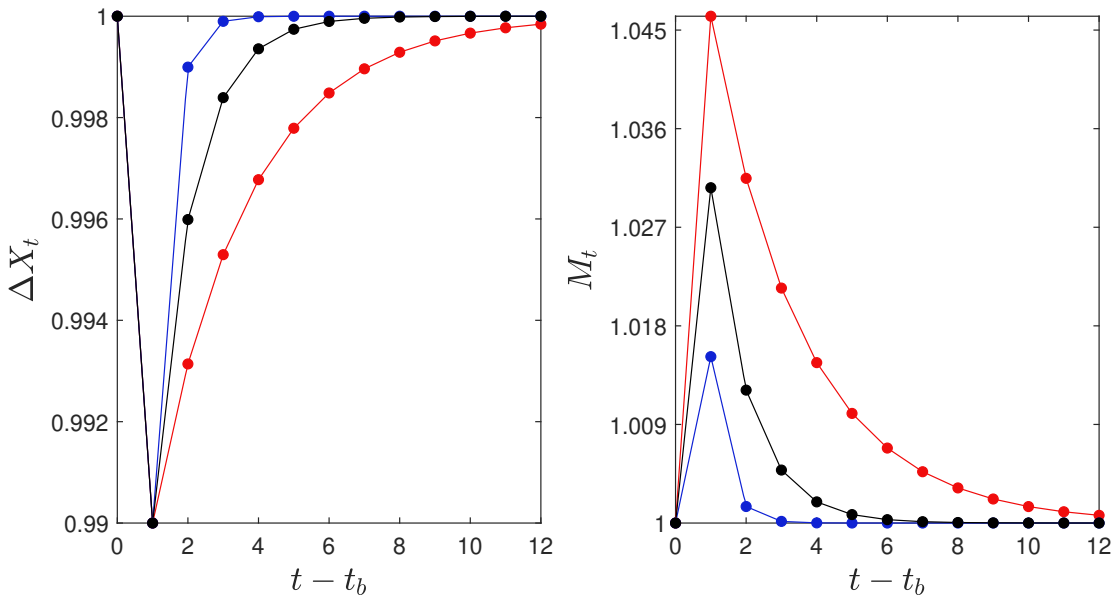

Figure 3: Dynamic Adjustment of Prices and Flows

This figure shows the adjustment process of oil supply X and oil price P for three scenarios: optimistic- (blue line), base- (black line) and pessimistic (red line) scenario.

[12]We note that there are a few cases with a regional supply shortage above 20%. In these cases, the shortage is capped. For more details, see section 4.2.

4 Data

4.1 Empirical trading network

We apply our theoretical commodity network model to data on physical oil flows from Refinitiv Eikon for Commodities. This database uses a variety of sources on the individual ship level including vessel position data (AIS), port authority information, and proprietary ship to ship data. Each vessel can be tracked around the globe using it's unique International Maritime Organization (IMO) number. For instance, on January 19, 2018, the vessel "CPO LARISA ARTEMIS" with IMO number 9305532 loaded 235,538 barrels of crude oil in Slagen, Norway and shipped it to Rotterdam in the Netherlands. Later that year, we observe the same vessel load 111,424 barrels of fuel oil in Algericas, Spain to ship it to Conakry in Guinea. We track 155,435 individual flows for the years 2007 - 2018 across time and space to generate a comprehensive map of physical commodity flows encompassing 5183 ports located in 90 load and discharge zones. The variables and their description are summarized in Table 2.

One of the main variables of interest is the commodity trader which chartered the vessel. Most commodity traders do not own a fleet of vessels but charter ships as needed from shipping companies. The concentration of traders within the market of global commodity flows provides valuable information concerning the market share and therefore potential systemic risk of individual traders. The contribution of individual large traders to the physical network of oil flows is discussed in more detail below. The cargo size measures the size of the shipment and determines the volume of aggregate flows between regions. The commodity type is in most cases crude oil but occasionally contains refined products such as gasoline or jet fuel. The freight rate is used to determine the shipping costs between locations and is contained in D_{ij}. Since shipping costs increase almost 1:1 with distance travelled, we use the distance in D_{ij} directly in the empirical part.

Based on the physical flows of crude oil and refined products, we construct an empirical trading network that forms the basis of our simulation study conducted in section 5. A common approach in the trading network research literature is to focus on so called backbone networks which are simplified versions of the original networks, retaining the basic

Variable Name	Description	Values
Charterer	The commodity trading company that charters the vessel for transportation	1,637 firms
IMO number	Unique identifier for each vessel	5,454 vessels
Cargo Size	Number of barrels carried by the ship	mean: 100,501 barrels sd: 84,529 barrels
Port	Load and discharge port	5,183 ports missing values:53%
Zone	Load and discharge zone for instance U.S. Gulf, Arabian Gulf, Mediterranean	90 zones missing values:13%
Commodity Type	Crude Oil, Fuel Oil, Naphtha Gas Oil, Gasoline, Jet Fuel	-
Freight Rate	Freight rate in % of World Scale Index	mean: 113% sd: 53%

Table 2: Description of Individual Ship Level Data

This table summarizes the variables that are available in the Refinitiv Eikon for Commodities data set. We observe 155,435 individual shipments of oil and refined oil products between 2007 and 2018.

network structures. Such a backbone network typically encompasses only the largest and most important trade flows, i.e. edges (see, e.g., Fair et al., 2017). For our study, we take a slightly different approach. On the one hand, we have to reduce the complexity of the empirical trading network such that it fits our theoretical model. On the other hand, due to the aim of our study, we have to keep as much trade flows for which a particular trader is responsible for as possible. As a compromise, we define a total of 15 major trading zones: 4 zones representing the Americas, 6 zones representing Europe, the Middle East and Africa (EMEA) and 5 zones representing Asia-Pacific (APAC). For each trader and each zone, we then calculate separately the average outflows and average inflows between 2007 - 2018. Aggregated flows are then obtained by summing over all traders as outlined in section 3.1.

For simplicity, we assume that each zone is comprised of one dedicated seller region and one dedicated buyer region, to which inflows and outflows can be assigned to. As an illustration, consider the two zones z_l and z_k. Let the dedicated seller regions of z_l and z_k be denoted by R_{l_1} and R_{k_1}, respectively. The corresponding buyer regions are R_{l_2} and R_{k_2}. Let aggregated flows from zone z_l to z_k be 8 million barrels (MMbbl) and the aggregates flows from z_k to z_l be 2 Mmbbl. We then set $X_{k_2l_1}$, measuring the flows from the seller region R_{l_1} to buyer region R_{k_2} to $X_{k_2l_1} = 8$. In constrast, the flows from seller region R_{k_1} to buyer region R_{l_2} are $X_{l_2k_1} = 2$. In line with our model, we abstract from trades within zones, i.e. $X_{k_1k_2} = X_{l_1l_2} = 0$.

The result of these steps is shown in Table 3. Note that trading zones with a positive net-flow are those typically regarded as oil importers, e.g. Europe, China and India, whereas trading zones with a negative net-flow are oil exporters such as the South America and the Middle East. Off course, in total, buyer region inflows match seller region outflows such that net-flows are zero. Further details regarding the sources and destinations of these flows are displayed in Figure C1.

4.2 Trader contribution

We next turn to the traders' contributions to the inflows and outflows shown in Table 3. The Gini coefficient measuring the dispersion of these trading volumes among the 1,637 traders is 0.96 which supports our claim that the commodity trading market is dominated by a relatively small number of very large traders. Even if we only consider the 100 largest traders, accounting for approximately 93% of all flows, we still get a Gini coefficient of 0.63. However, in order to make the simulation study in section 5 manageable, we further restrict the analysis to the 10 largest traders shown in Table 4. These companies account for a combined 43% of all flows.

A detailed overview of all outflows and inflows per company and region is provided in Table D2 and D3, respectively. We note that in only 2 out of 150 cases a trader's relative contribution exceeds 20%. UNIPEC is responsible for approximately 33 Mmbbl (47%) of China's and PETROBRAS for approximately 8 Mmbbl (45%) of South America's total seaborne inflows in a typical quarter over the sample period. One reason for these very large

	Trading zone	Buyer region flow	Seller region flow	Net-flow
Americas	Canada	8.41	-2.29	6.12
	Mexico	4.47	-20.85	-16.38
	South America	17.95	-32.93	-14.98
	USA	91.81	-56.04	35.77
EMEA	East Africa	10.37	-1.13	9.25
	North Africa	3.81	-29.74	-25.93
	West Africa	12.97	-155.1	-142.13
	Europe	202.85	-56.23	146.61
	Russia	0.17	-82.9	-82.73
	Middle East	14.15	-106.53	-92.37
APAC	China	71.95	-4.64	67.31
	India	51.93	-36.13	15.8
	Japan	17.75	-2.97	14.78
	Oceania	17.93	-11.24	6.69
	South Asia	101.35	-29.15	72.2
	Σ	627.87	-627.87	0.00

Table 3: Aggregate Oil Flows

This table shows the empirical Network of physical oil flows in million barrels (MMbbl) between zones within (*i*) the Americas, (*ii*) Europe, the Middle East and Africa (EMEA) and (*iii*) Asia-Pacific (APAC). All flows are based on annual averages for a sample period ranging from 2007 to 2018.

contributions is that some traders specialize on catering to a particular region of the world. For instance, Brazil's largest oil trading firm, the state-owned Petróleo Brasileiro S.A. or "PETROBRAS" manages predominantly oil flows to Brazil. A default of PETROBRAS is therefore estimated to cause large flow reductions in Brazil, but to have little quantity effects in other parts of the world.

Given our estimates for the price elasticity ϕ, a default of UNIPEC or PETROBRAS

Trader	Absolute	Cusum	Relative	Cusum
UNIPEC	42.35	42.35	6.75%	6.75%
SHELL	40.72	83.07	6.49%	13.23%
BP	36.33	119.40	5.79%	19.02%
VITOL	35.10	154.50	5.59%	24.61%
CNR	22.86	177.35	3.64%	28.25%
PETROBRAS	20.87	198.23	3.32%	31.57%
CSSSA	19.81	218.04	3.15%	34.73%
REPSOL	19.58	237.62	3.12%	37.85%
CLEARLAKE	16.87	254.48	2.69%	40.53%
ST SHIPPING	16.47	270.95	2.62%	43.15%

Table 4: The 10 Largest Commodity Traders by Flow Contribution
This Table shows the absolute (in Mmbbl) and relative contribution of the 10 largest traders to aggregated average buyer region inflows. Columns 3 and 5 show the respective cumulative sums (Cusum).

would translate in very large regional price jumps. However, a shock of this size would be likely to trigger regional land adjustment processes in which oil is transported on road and rail in an emergency response. In this paper, we concentrate on economically large but still realistic flow reductions and introduce a supply reduction cap of 20% of the long-run values. When setting a cap on the size of the inflow reductions at some buyer region, we adjust the flow of all seller regions according to their relative contribution. The results of this procedure are provided in Tables D4 and D5 with adjusted out- and inflows indicated by bold numbers. Further details regarding these calculations are provided Appendix A.3

5 Simulation of Trader Bankruptcy

The bankruptcy of a trader results in the removal of that firm from the network of long-run commodity flows. We introduce a shock in period t_b that leads to a disruption of all flows operated by the bankrupt trader. The impact of this shock on commodity prices in buyer region R_i at time $t \geq t_b$ is measured by the relative price increase

$$\pi_{i,t} = \frac{P_{i,t}}{\overline{P}_i} - 1 \tag{13}$$

where local commodity prices in the i-th region $P_{i,t}$ are weighted averages of the export prices over all trading partners:

$$P_{i,t} = \sum_{j=1}^{K} \alpha_{ij,t} P_{ij,t}. \tag{14}$$

The weight $\alpha_{ij,t}$ should reflect the size of the trading relationship between R_i and R_j at time t and is hence defined as $\alpha_{ij,t} = X_{ij,t}/X_{i,t}$. Over time, the affected regions accommodate the shock so that $P_{i,t} \to \overline{P}_i = \sum_{j=1}^{K} \overline{\alpha}_{ij} \overline{P}_{ij}$ and $\pi_{i,t} \to 0$ as $(t - t_b) \to \infty$ where $\overline{\alpha}_{ij} = \overline{X}_{ij}/\overline{X}_i$ is the long-run trading weight.

Note that the measure $\pi_{i,t}$ does not depend on global commodity price levels G: Because $P_{ij,t} = GD_{ij}M_{i,t}$ and $\overline{P}_{ij} = GD_{ij}$, Equation (13) can be rewritten as

$$\pi_{i,t} = M_{i,t} w_{i,t} - 1 \tag{15}$$

where $w_{i,t} = \sum_{j=1}^{K} a_{ij,t} D_{ij} / \sum_{j=1}^{K} \overline{a}_{ij} D_{ij}$. Equation (15) highlights two transmission channels from the failure of a commodity trader on local commodity prices. First, prices respond to the size of the local supply shock as measured by the margin multiplier $M_{i,t}$, and second, prices depend on the specific network structure of trade links as measured by $w_{i,t}$. However, the main source of the price response is due to the margin multiplier $M_{i,t}$ which explains 96% to 99% of the variation of $\pi_{i,t}$.[13]

In the next section 5.1, we provide a ranking of the top 10 traders with respect to their systemic risk based on the absolute import reduction and price response measures π. In section 5.2, we further analyse the dynamics π for the three scenarios provided in Table 1,

[13] An alternative specification with equal distances $D_{ij} = D$ for all i, j generates very similar results. In the following, however, we retain the more realistic distance matrix based on actual kilometer distances.

whereas total payment flows from the seller and the buyer region's perspective are explored in in section 5.3.

5.1 Trader Ranking

The price and quantity dynamics that unfold over a period of 5 quarters after the shock in the base scenario are shown in Figure 4. Panel A shows the reductions in flows. We consider again PETROBRAS, the large Brazilian oil trader that focuses primarily on supplying South America with energy. A simulated default is estimated to reduce flows to South America by 4 million barrels, which corresponds to a relative supply gap of 20%. The corresponding price response shown in Panel B is economically large and estimated to be 95% in the first quarter and 31% in the second quarter. As competing oil traders reorganize to fill the supply gap of PETROBRAS, physical trade flows and prices return to pre-shock levels starting from the third quarter. To put the size of a 4 million barrel shock into economic perspective, we refer to simulation results from Inoue and Todo (2022) who quantify the size of import disruption on the real economy in Japan. The majority of empirical evidence on supply chain disruptions within a country is collected for Japan because the data on the industry structure of Japanese firms offers a particularly detailed set of industry linkages that allow for such an analysis. Inoue and Todo (2022) estimate that a $1 import disruption from Middle Eastern countries to Japan results in a $3.12 reduction in economic production. If we assume that imports from the Middle East consist mainly of oil and that oil prices are $80 per barrel, a 4 million import reduction is worth $320m which would reduce economic production by $1bn in the first quarter of the shock or 0.62% of Brazilian GDP. The joint failure of more than one large commodity trader could amplify this effect.

From Panel B we conclude that the forced removal of a commodity trader from the long-run network of firms will have considerable local price effects that can extend over two quarters if the region receives the majority of imports through the defaulted trader. More generally, simulated commodity prices are more elastic than quantities, an observation that is confirmed by empirical studies, notably Baumeister and Peersman (2013a).

The price and quantity responses following the default of a commodity trading firm

allows us to rank traders in decreasing order of systemic risk. Table 5 is inspired by the systemic risk ranking of financial institutions that is reported and updated by the V-Lab of New York University.[14] Our ranking reflects the impact that the default of a commodity trader exercises on both supply shortages as well as prices. The position in the overall ranking is determined by the average over both indicators. For instance, the supply shortage resulting from a default of Shell is estimated as the average weighted import reduction across all regions that receive imports from Shell over a period of 5 quarters. In particular, the default of Shell is estimated to reduce imports in the target regions United States, South Asia, and Europe on average by 10.77 million barrels per quarter. While Shell is ranked 1st in terms of supply impact, it is not estimated to have the largest price impact with prices in the three target regions estimated to be 6.5% above their long-run values that occur in the absence of any shock. The top 10 systemically important US financial firms include names like Citigroup, JP Morgan, and Bank of America, our list features Shell, BP, and Vitol as systemically important commodity firms.

[14] See NYU Stern V-Lab

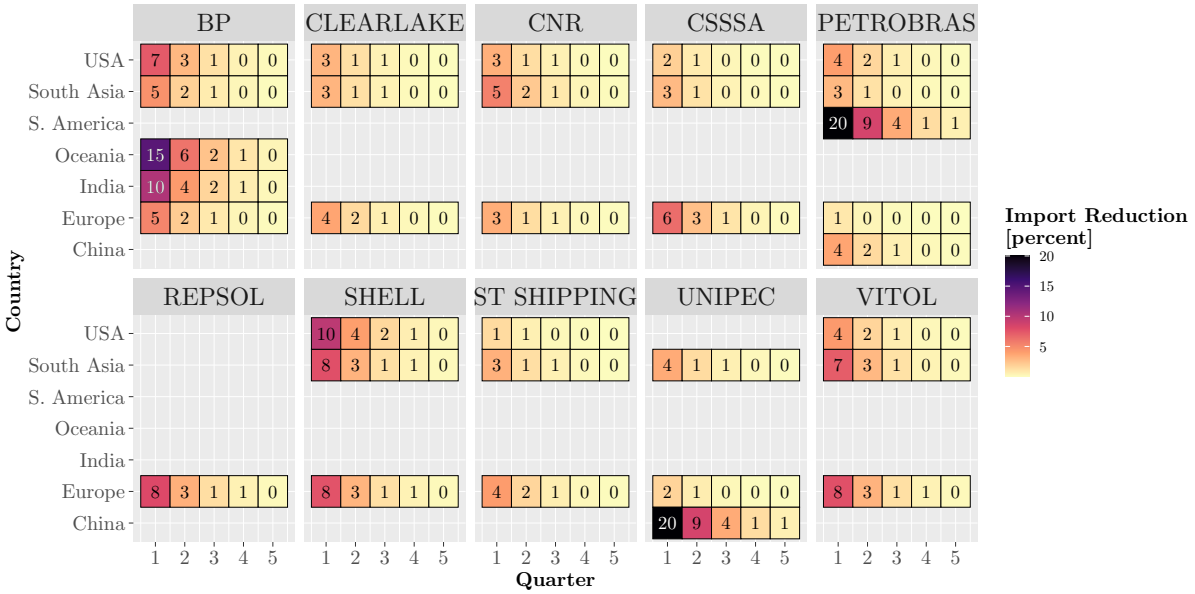

(**A**) Import Reductions

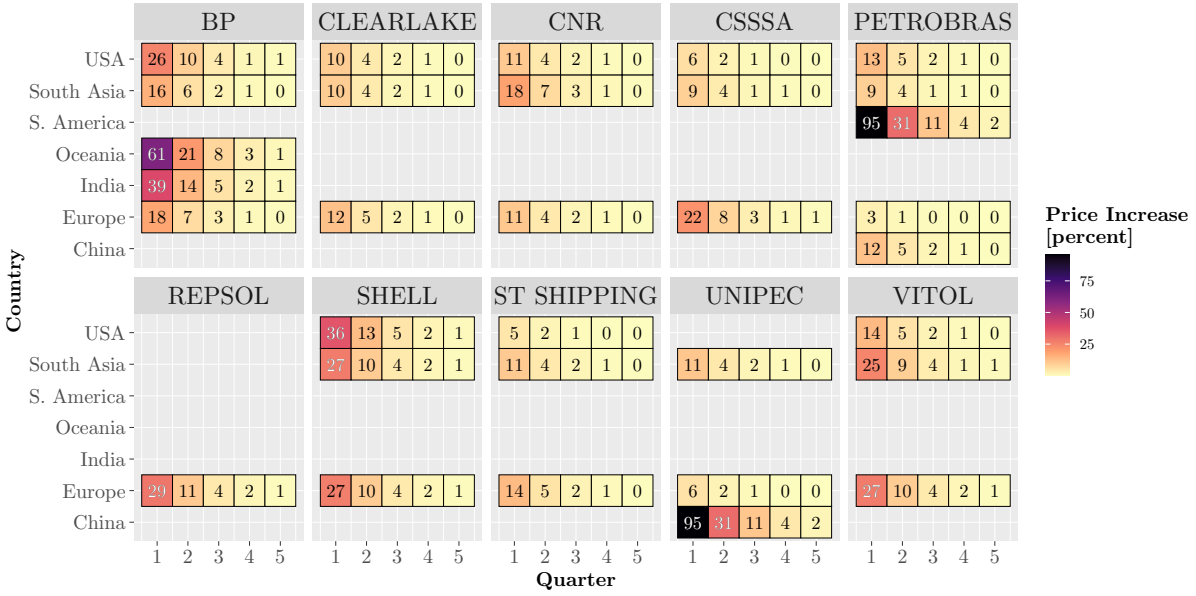

(**B**) Price Response

Figure 4: Simulated Quantity and Price Effects from Trader Default

This figure shows simulated outcomes following the default of a large commodity trading firm. Panel A highlights the regional focus of oil trading firms and the reductions in oil flows following the failure of a trader. Panel B shows the price increases that are associated with the supply disruption. The price elasticity calibrated from our data is larger than the demand elasticity.

Import Reduction (in MMbbl)	Price Impact π (in %)	Ranking
10.77	6.50	SHELL
8.96	7.45	VITOL
10.10	6.32	BP
5.47	9.15	REPSOL
7.29	7.06	UNIPEC
5.92	4.04	CSSSA
5.15	4.32	CNR
4.53	3.48	CLEARLAKE
4.96	2.75	PETROBAS
4.37	3.12	ST SHIPPING

Table 5: Commodity Trader Ranking

This table ranks the commodity trading firms in our sample according to systemic risk in the base scenario. The ranking is determined by accounting for the size in import reductions (in million barrels per quarter) and for price effects (in percent relative to equilibrium). The price averages are weighted based on flow size, i.e. buyer regions that receive higher flows also have a higher price weight. The position of a trader in this table is determined by the average over both indicators.

5.2 Scenario Analysis

The empirical results discussed so far depend on estimates under a base scenario of price and quantity adjustment parameters. The parameter ϕ governs the price elasticity of a supply disruption and was estimated to be 3 on average while ψ reflects the size of trader's response to the resulting supply gap and was estimated to be 0.2. However, the ability of the remaining traders to respond to the supply shortages left by a defaulted trader depends on the risk appetite and the funds available to take over parts of the business of the defaulted competitor. For instance, the fleet of vessels that are no longer managed by

the defaulted trader requires a team of ship operators and other supporting staff in order to commence trading in the pre-shock form. Figure 5 shows three scenarios that illustrate this point. In the optimistic scenario, the price response due to a trader's default, measured by the parameter ϕ, is lower than in our base scenario while the adjustment parameter ψ is higher ($\phi = 1.5$ and $\psi = 0.6$). In this optimistic scenario, the price impact is muted and supply shortages are quickly adjusted by the remaining traders. However, the circumstances in which a commodity trader goes bankrupt are likely to occur in a financially stressful environment for commodity traders in general. After all, commodity traders often trade the same commodities. It is therefore quite likely that the circumstances that led to the default of a trader in the first place, reduce the funds available as well as the risk appetite of the remaining traders, which complicates the takeover of the defaulted team and can prolong the adjustment process. This case is illustrated in the pessimistic scenario in which the price response from the same shock is larger ($\phi = 4.5$) while the ability of traders to respond to the supply gap is subdued ($\psi = 0.07$).

Panel A shows absolute price and quantity responses. Average oil imports are estimated to be lower by 25 million barrel in the quarter following the shock with local prices up by 5$ - 10$. Panel B shows price and quantity responses in relative terms and highlights that the price effect is dominating the quantity effect. This reflects the generally low price elasticity of oil demand in the economy (Cooper, 2003) as well as the functioning of the remaining network of commodity imports.

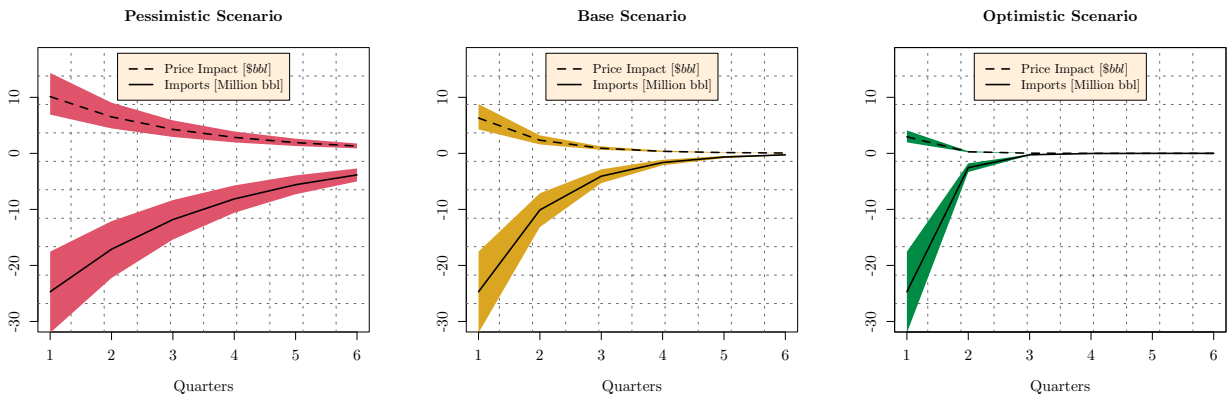

(**A**) Absolute Changes

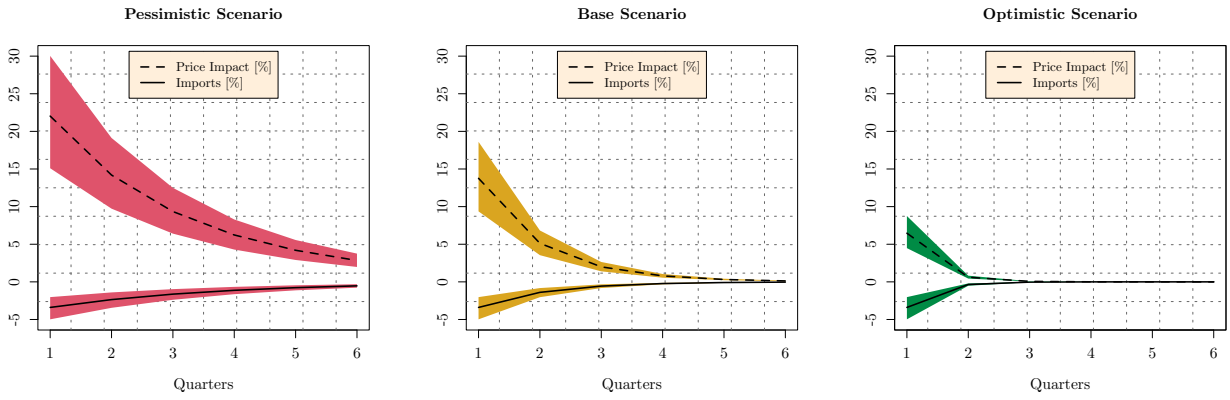

(**B**) Relative Changes

Figure 5: This figure shows post-shock import flow and price dynamics for three different scenarios. In the pessimistic scenario the supply shortage has a large price effect ($\phi = 4.5$) and the speed with which commodity traders are able to close the supply gap is low ($\psi = 0.07$). These parameters are subsequently relaxed for the following scenarios with the optimistic scenario assuming small price jumps ($\phi = 1.5$) and flexible remaining traders who can quickly respond to the default ($\psi = 0.6$). The solid and dashed lines are generated from weighted averages across all regions. The upper and lower bands correspond to the 75% and 25% quantile of the price and flow distribution.

5.3 Payment Flows

So far, we have highlighted the dependency of importing regions on a functioning supply chain of natural resources. However, commodity deposits are not randomly distributed in the earth's crust but are instead concentrated in a few regions of the world. These regions strongly depend on the revenues of commodity exports to balance their budgets and finance their government expenditures. In this section, we therefore briefly turn to the payment flows that mirror the commodity flows.

Recall that financial flow $C_{ij,t}$ as defined in Equation (4) can be interpreted as either seller region R_j's revenue or the buyer region R_i's import costs. Here, we consider both perspectives and begin with the seller region. Total payment flows collected at such a region R_j are obtained by aggregating over all buyers R_i. Let therefore $C_{\cdot j,t} = \sum_{i=1}^{j} C_{ij,t}$ be the short-run income and $\overline{C}_{\cdot j} = \sum_{i=1}^{j} \overline{C}_{ij}$ be its long-run counterpart. The relative time t deviation from long-run income is thus

$$\chi_{\cdot j,t} = \frac{C_{\cdot j,t}}{\overline{C}_{\cdot j}} - 1. \tag{16}$$

Oil export revenues for one region mean import costs for another region. Buyer region R_i's short- and long-run import costs $C_{i\cdot,t}$ and $\overline{C}_{i\cdot}$ are obtained by aggregating over all sellers R_j. The relative time t deviation from long-run import costs is consequently $\chi_{i\cdot,t} = C_{i\cdot,t}/\overline{C}_{i\cdot} - 1$.

The failure of a large commodity trader constitutes a transitory shock that increases prices and boosts export revenues for exporting regions while at the same time generating higher costs and lower real incomes for households in importing regions. Figure 6 illustrates the estimated percentage changes in export revenues $\chi_{\cdot j,t}$ and import costs $\chi_{i\cdot,t}$ after the bankruptcy of BP or Shell. To conserve space, we concentrate on these two large commodity trading firms but other traders have similar effects. The left panel highlights that oil exporting regions can increase their export revenues by 20% and more relative to an equilibrium situation in which no shock occurred. On the other hand, the right panel shows higher import costs for importing regions with specific regions such as East Africa and Australia being exposed to 50% higher import costs when BP, an important trader for this regions, would suddenly become unable to deliver crude oil. Figure 6 highlights large commodity traders have the potential to have significant adverse effects on the trade balance and income of most regions in the world.

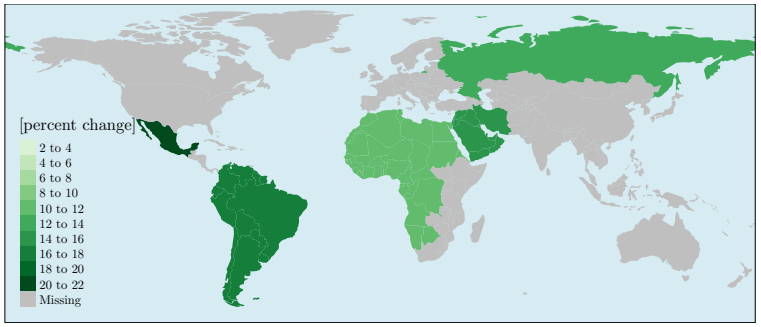

(**A**) Export Revenues after BP Shock

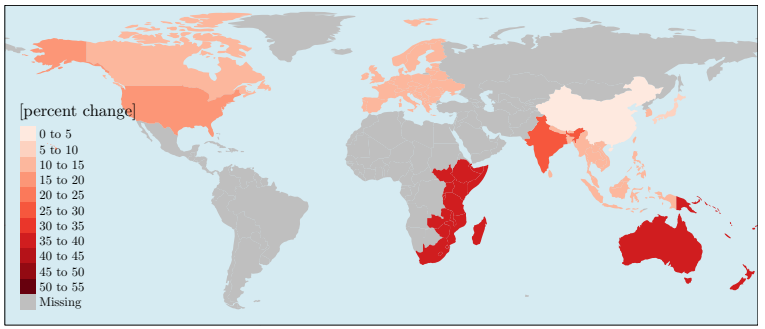

(**B**) Import Costs after BP Shock

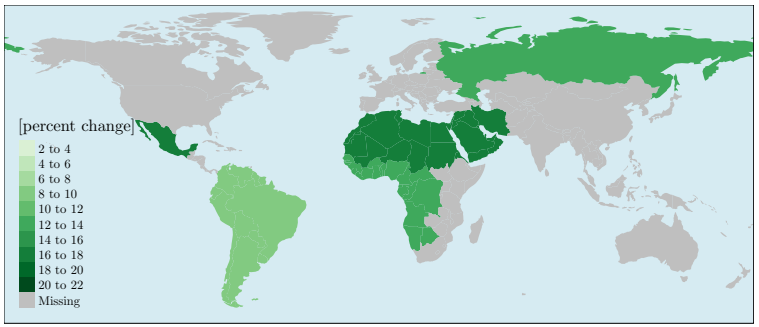

(**C**) Export Revenues after Shell Shock

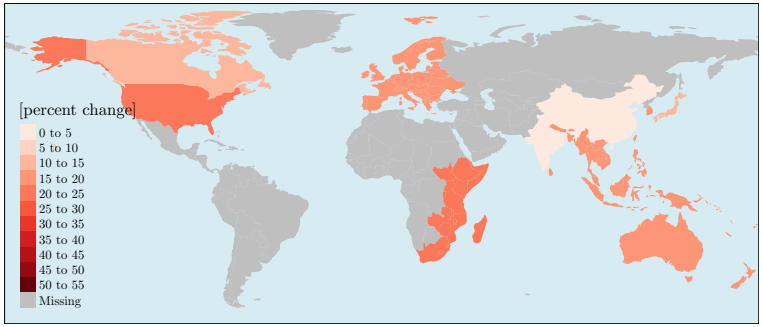

(**D**) Import Costs after Shell Shock

Figure 6: Export Revenues and Import Costs after Trader Bankruptcy

Panel A and C on the left show the estimated percentage increase in oil exports $\chi_{\cdot j,t}$ following the bankruptcy of BP or Shell. Oil exporting regions will generally benefit from higher oil prices and can increase their export revenues by more than 20% relative to their long-run values. Higher export revenues for exporting regions mean higher import costs $\chi_{i\cdot,t}$ for importing regions as shown on the right side of the figure in Panel B and D. East Africa and Australia appear to be particularly vulnerable to a scenario in which BP would no longer be able to deliver crude oil with import costs increasing to more than 50% during the first quarter of the shock.

6 Conclusion

Commodity trading firms are responsible for the timely delivery of energy commodities, building materials, and other natural resources that are used in the production of economic activity. A survey conducted in 2022 reports that more than half of European firms had encountered disruptions to deliveries due to shipping delays (Javorcik et al., 2022). In February 2023, Trafigura booked a $600m loss after discovering that cargoes of nickel were in fact worthless stones. Germany and Italy agreed to guarantee loans to the Singapore based Trafigura to reduce risks for its creditors and ensure a smooth supply of raw materials (Economist, 2023). In this paper, we argued that the failure of a commodity trader can cause supply disruptions that propagate to other sectors of the economy. In other words, commodity trading firms are systemically important. So far, commodity trading firms have shown remarkable resilience and bankruptcy is not observed in the data. We therefore turn to simulation results to address our research question. We propose a trading network model of physical commodity flows that simulates the response of the remaining traders after the bankruptcy event. Based on empirically calibrated adjustment coefficients, we estimate that the failure of one of our top ten systemically important traders has significant effects on local prices and supply. According to our estimations, regions that share trade links with the affected energy trader can experience local supply disruptions with prices doubling in the following quarter and supply cuts of up to 20%. The time dynamics following the trader bankruptcy depend on the speed of adjustment with which the remaining network of traders can accommodate the trade gap. In our pessimistic scenario that is based on the assumption that the remaining network lacks the capacity to take over major parts of the failed company, prices and supply take more than one year to return to the pre-shock equilibrium. Our results indicate that commodity trading firms are systemically relevant but that the economic mechanism is different for commodity traders than for financial institutions.

Private ownership allows commodity trading firms to operate in environments that include opaque ownership structures, unstable governments, and war zones. But it also generates an environment in which commodity traders have become systemically important without the notice of investors and regulators. Given that energy security is one of the top

priorities of policy makers in Europe, our paper highlights an important mechanism that has so far been underappreciated. The literature on global supply chains offers two main recommendations for improving the robustness and resilience of global trade links: First, diversification of global supply chains has been shown to reduce the volatility of economic activity (D'Aguanno et al., 2021; Baldwin and Freeman, 2022). Second, Stockpiling and inventory management increases costs for individual firms but provides a much needed buffer during suply shocks (Kamalahmadi and Parast, 2016; Martins Sa et al., 2019). In line of these findings, we argue that a reshuffling of commodity supply chains can also help to mitigate the effects from disruptions due to commodity trader defaults. Affected regions can adapt by increasing physical storage of inputs and by diversifying their base of suppliers and commodity trading firms.

References

Acemoglu, D., V. Carvalho, A. Ozdaglar, and A. Tahbaz-Salehi. (2012). The network origins of aggregate fluctuations. *Econometrica*.

Acharya, V. V., L. H. Pedersen, T. Philippon, and M. Richardson (2017). Measuring systemic risk. *The Review of Financial Studies*.

Adrian, T. and M. K. Brunnermeier (2016). Covar. *American Economic Review*.

Baines, J. and S. Hager (2021). Commodity traders in a storm: financialization, corporate power and ecological crisis. *Review of International Political Economy*.

Baldwin, R. and R. Freeman (2022). Risks and global supply chains: What we know and what we need to know. *Annual Review of Economics 14*, 153–180.

Barrot, J.-N. and J. Sauvagnat (2016). Input Specificity and the Propagation of Idiosyncratic Shocks in Production Networks. *The Quarterly Journal of Economics*.

Baumeister, C. and G. Peersman (2012). Appendix to: The role of time-varying price elasticities in accounting for volatility changes in the crude oil market. *Journal of Applied Econometrics*.

Baumeister, C. and G. Peersman (2013a). The role of time-varying price elasticities in accounting for volatility changes in the crude oil market. *Journal of Applied Econometrics*.

Baumeister, C. and G. Peersman (2013b). Time-varying effects of oil supply shocks on the us economy. *American Economic Journal: Macroeconomics*.

Bernard, A. B. and A. Moxnes (2018). Networks and trade. *Annual Review of Economics 10*(1), 65–85.

Blanchard, O. and M. Riggi (2013). Why are the 2000s so different from the 1970s? a structural interpretation of changes in the macroeconomic effects of oil prices. *Journal of the European Economic Association*.

Carvalho, V. M., M. Nirei, Y. U. Saito, and A. Tahbaz-Salehi (2020). Supply Chain Disruptions: Evidence from the Great East Japan Earthquake. *The Quarterly Journal of Economics 136*.

Cooper, J. C. (2003). Price elasticity of demand for crude oil: estimates for 23 countries. *OPEC Review 27*(1), 1–8.

D'Aguanno, L., O. Davies, A. Dogan, R. Freeman, S. Lloyd, D. Reinhardt, R. Sajedi, and R. Zymek (2021). Global value chains, volatility and safe openness: Is trade a double-edged sword? *Bank of england financial stability paper* (46).

Economist, T. (2023). Why commodity-trading scandals are multiplying. *The Economist*. https://www.economist.com/finance-and-economics/2023/04/27/why-commodity-trading-scandals-are-multiplying?giftId=1486f5d1-9929-4b06-8d0d-79b7a2fab54d.

Eggert, N., G. Ferro-Luzzi, and D. Ouyang (2017). Commodity trading monitoring report. *Swiss Research Institute on Commodities*.

Engle, R. (2018). Systemic risk 10 years later. *Annual Review of Financial Economics*.

Fair, K., C. Bauch, and A. Madhur (2017). Dynamics of the global wheat trade network and resilience to shocks. *Nature Scientific Reports*.

Foti, N., S. Pauls, and D. Rockmore (2013). Stability of the world trade web overtime – an extinction analysis. *Journal of Economic Dynamics and Control*.

Gabaix, X. (2011). The granular origins of aggregate fluctuations. *Econometrica*.

Gilbert, C. (2021). Monopolistic supply management in world metals markets: How large was mount isa? *Journal of Commodity Markets*.

Goldberg, P. K. and T. Reed (2020). Income distribution, international integration, and sustained poverty reduction. Technical report, National Bureau of Economic Research.

Inoue, H. and Y. Todo (2022). Propagation of overseas economic shocks through global supply chains: Firm-level evidence. *Available at SSRN 4183736*.

Jackson, M. and A. Pernoud (2021). Systemic risk in financial networks: A survey. *Annual Review of Economics*.

Javorcik, B., L. Kitzmüller, and H. Schweiger (2022). Business unusual: Global supply chains in turbulence. Technical report, European Bank for Reconstruction and Development Transition Report 2022-23.

Kamalahmadi, M. and M. M. Parast (2016). A review of the literature on the principles of enterprise and supply chain resilience: Major findings and directions for future research. *International Journal of Production Economics 171*, 116–133.

Kang, W., K. Tang, and N. Wang (2023). Financialization of commodity markets ten years later. *Journal of Commodity Markets*.

Kilian, L. (2009). Not all oil price shocks are alike: Disentangling demand and supply shocks in the crude oil market. *American Economic Review*.

Kilian, L. (2014). Oil price shocks: Causes and consequences. *Annual Review of Resource Economics*.

Kilian, L. and D. Murphy (2014). The role of inventories and speculative trading in the global market for crude oil. *Journal of Applied Econometrics*.

Liu, L., Z. Cao, X. Liu, L. Shid, S. Cheng, and G. Liu (2020). Oil security revisited: An assessment based on complex network analysis. *Energy*.

Lütkepohl, H. and A. Netšunajev (2014). Disentangling demand and supply shocks in the crude oil market: How to check for sign restrictions in structural vars. *Journal of Applied Econometrics*.

Martins Sa, M., P. de Souza Miguel, R. de Brito, and S. Farias Pereira (2019, April). Supply chain resilience: the whole is not the sum of the parts. *International Journal of Operations and Production Management 40*(1), 92–115.

Oomes, N., B. Tieben, A. Laven, T. Ammerlaan, R. Appelman, C. Biesenbeek, and E. Bunk (2016). Market concentration and price formation in the global cocoa value chain. *SEO-rapport* (2016-79).

Ritchie, H., M. Roser, and P. Rosado (2022). Energy. *Our World in Data*. https://ourworldindata.org/energy.

Wei, N., X. Wen-Jie, and Z. Wei-Xing (2022). Robustness of the international oil trade network under targeted attacks to economies. *Energy*.

Appendix A Proofs and Additional Remarks

A.1 Proof of Proposition 1

We begin with the inequality for the capacity multiplier $0 < \kappa < 1$ which can be shown by induction. For an arbitrary t, assume that $\Delta X_{i,t} < 1$. In this case, $M_{i,t}^{\psi} > 1$ which yields

$$0 < \left(M_{i,t}^{\psi} - 1\right) \Delta X_{i,t} \tag{A.1}$$

Furthermore, because $0 < \phi\psi < 1$, we get $M_{i,t}^{\psi} \Delta X_{i,t} = \Delta X_{i,t}^{(1-\phi\psi)} < 1$ and thus

$$\left(M_{i,t}^{\psi} - 1\right) \Delta X_{i,t} = \Delta X_{i,t}^{(1-\phi\psi)} - \Delta X_{i,t} < 1 - \Delta X_{i,t} \tag{A.2}$$

Together, Inequalities (A.1) and (A.2) imply $0 < \kappa_{i,t} < 1$. Now, because $\Delta X_{i,t} < 1$, there is at least one seller j^* with $\Delta X_{ij^*,t} < 1$. Because $0 < \kappa_{i,t} < 1$, Equation (9) implies $\Delta X_{ij^*,t+1} < 1$ and thus $\Delta X_{i,t+1} < 1$. In particular, we have $\Delta X_{i,t_b} < 1$ at shock time t_b by definition. Hence, $\Delta X_{i,t} < 1$ and thus $0 < \kappa_{i,t} < 1$ holds for all $t \geq t_b$.

Next, we consider the dynamics of relative supply. Multiplying both sides of Equation (9) by long-run seller j supply $\overline{X}_{ij}$ and summing over all sellers j yields

$$X_{i,t+1} = X_{i,t} + \kappa_{i,t} \left(\overline{X}_i - X_{i,t}\right) \tag{A.3}$$

Similarly, by multiplying numerator and denominator of the right side of Equation (10) by total long-run supply $\overline{X}_i$ we obtain

$$\kappa_{i,t} = \frac{\left(M_{i,t}^{\psi} - 1\right) X_{i,t}}{\overline{X}_i - X_{i,t}}. \tag{A.4}$$

Inserting Equation (A.4) in (A.3) yields total supply dynamics $X_{i,t+1} = X_{i,t} M_{i,t}^{\psi}$ which is equivalent to relative supply dynamics $\Delta X_{i,t+1} = \Delta X_{i,t} M_{i,t}^{\psi}$ and thus $\Delta X_{i,t+1} = \Delta X_{i,t}^{(1-\phi\psi)}$.

Regarding the limits of ΔX and κ, we first note that we can rewrite the time $t \geq t_b$ buyer region i relative supply $\Delta X_{i,t}$ as a function of the shock at t_b, i.e.

$$\Delta X_{i,t} = \Delta X_{i,t_b}^{(1-\phi\psi)^{(t-t_b)}}. \tag{A.5}$$

Because $0 < \phi\psi < 1$, we have $(1 - \phi\psi)^{(t-t_b)} \to 0$ and thus $\Delta X_{i,t} \to 1$ as $(t - t_b) \to \infty$. In case of a specific seller region j with $X_{ij,t_b} < \overline{X}_{ij}$, we note that Equation (9) implies

$\Delta X_{ij,t} < 1$ for all $t \geq t_b$, i.e. there is no seller with short- or long-run oversupply. Hence, full supply $\Delta X_{i,t} \to 1$ is possible only if for each seller $\Delta X_{ij,t} \to 1$. Finally, regarding the capacity multiplier, we first rewrite Equation (10) by replacing $M_{i,t}^{\psi} \Delta X_{i,t}$ with $\Delta X_{i,t}^{(1-\phi\psi)}$:

$$\kappa_{i,t} = \frac{\Delta X_{i,t}^{(1-\phi\psi)} - \Delta X_{i,t}}{1 - \Delta X_{i,t}}. \tag{A.6}$$

Both, numerator and denominator of Equation (A.6) approach zero as $\Delta X_{i,t} \to 1$ so we can apply l'Hospital's rule which yields $\kappa_{i,t} \to \phi\psi$ as $\Delta X_{i,t} \to 1$.

A.2 Properties of the capacity multiplier κ

The left panel of Figure A1 plots κ_t and its approximation $\tilde{\kappa} = \phi\psi$ for a relative supply shortage below or equal to 20%. As can be seen, κ is well approximated by $\tilde{\kappa}$ in all three scenarios. The right panel shows the relative deviation of κ from $\tilde{\kappa} = \phi\psi$. In all three scenarios, this relative deviation is below 8.2%.

A.3 Capped in- and outflows

We demonstrate the procedure of capping in- and outflows in case of PETROBRAS. As shown in Table D3, about 8.032 Mmbbl inflows to South America are assigned to this trader. Total inflows to South America are 17.95 Mmbbl, so PETROBRAS is responsible for about

$$8.032/17.95 \approx 45\%.$$

In order to cap the reduction of inflows to South America caused by the bankruptcy of PETROBAS, we reduce its contribution by 4.44 Mmbbl, such that

$$(8.032 - 4.44)/17.95 \approx 20\%.$$

The new capped inflows of $8.032 - 4.44 = 3.59$ Mmbbl to South America that are assigned to PETROBRAS are shown in Table D5.

The reduction of inflows has to be mirrored in the associated outflows. For example, 5.46 Mmbbl of all outflows assigned to PETROBRAS originate from West Africa (see

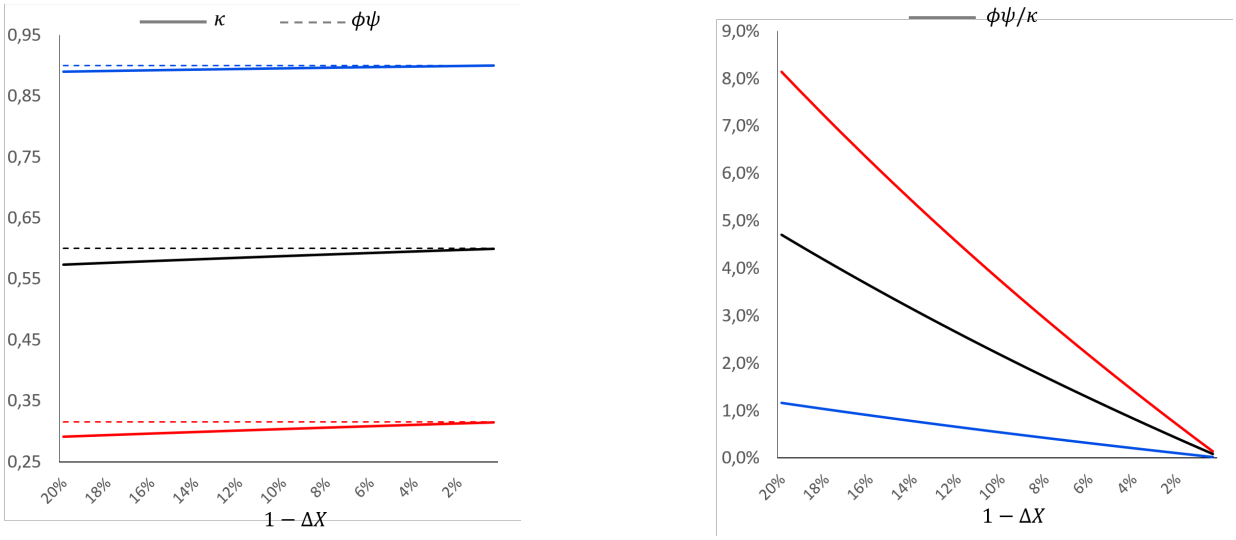

(A) Absolute values

(B) Relative deviation

Figure A1: Panel (A) shows the capacity multiplier κ as a function of the supply shortage $1 - \Delta X$. The blue line shows κ in case of $\phi = 1.5$ and $\psi = 0.6$ (optimistic scenario). The black line shows κ in case of $\phi = 3.0$ and $\psi = 0.2$ (base scenario). The red line shows κ in case of $\phi = 4.5$ and $\psi = 0.07$ (pessimistic scenario). The dotted lines are respective limits of κ given by $\phi\psi$. Panel (B) shows the corresponding relative deviation $\phi\psi/\kappa - 1$.

Table D2) from which about 4.28 Mmbbl are shipped to South America. West Africa is thus responsible for

$$4.28/8.032 \approx 53\%$$

of all uncapped South American inflows via PETROBRAS. In order to maintain this proportion in case of the capped inflows, we reduce West African outflows by $4.44 \cdot 53\% = 2.37$ Mmbbl such that again

$$(4.28 - 2.37)/3.59 \approx 53\%$$

of all West African outflows are shipped to South America. Consequently, total West African outflows of 5.46 Mmbbl assigned to PETROBRAS have to be reduced by 2.37 Mmbbl yielding the capped outflows of $5.46 - 2.37 = 3.08$ Mmbbl shown in D4.

Appendix B Model-Parameter Estimation

B.1 VAR-Model and IRFs

Baumeister and Peersman (2013a,b) define a VAR(4)-model with time-varying parameters and stochastic volatility for the data vector $y_t = (\delta x_t, \delta p_t, \delta q_t)'$, containing log differences of quarterly measures for global oil production, U.S. Crude Oil import prices and world industrial production, respectively. The structural form of this VAR is

$$B_{0,t}^{-1} y_t = c_t^* + \sum_{i=1}^{4} B_{i,t}^* y_{t-i} + \varepsilon_t \tag{B.1}$$

where $\varepsilon_t \sim N(0, I_3)$. Matrix $B_{0,t}^{-1}$ represents the time t instantaneous relationships between the elements of y_t. The corresponding reduced form model is

$$y_t = c_t + \sum_{i=1}^{4} B_{i,t} y_{t-i} + u_t \tag{B.2}$$

where $c_t = B_{0,t} c_t^*$, $B_{i,t} = B_{0,t} B_{i,t}^*$ and $u_t = B_{0,t} \varepsilon_t$. By assumption, $u_t \sim N\left(0, A_t^{-1} H_t (A_t^{-1})'\right)$, where A_t is a 3×3 a lower triangular matrix with ones on the main diagonal and non-zero off-diagonal elements and H_t is a 3×3 diagonal matrix. Regarding the time dependency, let $a_t = (a_{21,t}, a_{31,t}, a_{32,t})'$ be the vector containing the elements below the main diagonal of A_t, $h_t = (h_{1,t}, h_{2,t}, h_{3,t})'$ be the vector containing the main diagonal elements of H_t and $\theta_t = \text{Vec}(c_t, B_{1,t}, \ldots, B_{4,t})$.[15] The vectors θ_t and a_t are modeled as independent driftless random walks whereas $\log(h_t)$ is modeled as independent geometric random walk.

Due to its flexible structure, fitting this model to the data is somewhat more involved. Baumeister and Peersman (2013a,b) suggest to use Bayesian methods and a Markov Chain Monte Carlo Algorithm. A discussion of these methods as well as the approach to reconstruct $B_{0,t}$ is beyond the scope of this paper. For an excellent overview, we refer to Baumeister and Peersman (2012). Once model parameters are estimated, however, generating IRFs for the forecasting period $t+1$ to $t+h$ based on the relevant observations up to time t, i.e. $y_{t-3}, ..., y_t$, is straightforward and involves the following four steps:

[15] The Vec operator stacks the columns of a $m \times n$ matrix into an $mn \times 1$ vector. Here, θ_t is 39×1.

Step 1: Generate R parameter sets $\Psi_{r,t} = (\theta_{r,t+1}, ..., \theta_{r,t+h}, a_{r,t+1}, ..., a_{r,t+h}, h_{r,t+1}, ..., h_{r,t+h})$, each representing a different state of the economy from $t+1$ to $t+h$. These parameter sets are obtained by random draws from the respective estimated parameter distributions.

Step 2: For each $\Psi_{r,t}$, generate N different benchmark and shock forecast series based on $y_{t-3}, ..., y_t$ via Equation (B.2), i.e.

$\hat{y}^{(B)}_{r,n,t+1}, ..., \hat{y}^{(B)}_{r,n,t+h}$ (n'th benchmark forecast series for the r'th state),

$\hat{y}^{(S)}_{r,n,t+1}, ..., \hat{y}^{(S)}_{r,n,t+h}$ (n'th shock forecast series for the r'th state).

A difference between benchmark and shock forecasts is obtained via the reduced form innovations in Equation (B.2). In case of the benchmark series, innovations are $u^{(B)}_{t+1}, ..., u^{(B)}_{t+h}$ whereas in case of the shock series innovations are $u^{(S)}_{t+1}, ..., u^{(S)}_{t+h}$. These innovations are generated as follows: At time $t+1$, randomly draw ϵ_1, ϵ_2 and ϵ_3 from a standard normal distribution, calculate

$$u^{(B)}_{t+1} = B_{0,t+1}(\epsilon_1, \epsilon_2, \epsilon_3)', \tag{B.3}$$

$$u^{(S)}_{t+1} = B_{0,t+1}(\epsilon_1 - 1, \epsilon_2, \epsilon_3)'. \tag{B.4}$$

and check following sign restrictions:

(i) $u^{(S)}_{1,t+1} - u^{(B)}_{1,t+1} < 0$ (time $t+1$ oil supply growth is lower in the shock series)

(ii) $u^{(S)}_{2,t+1} - u^{(B)}_{2,t+1} > 0$ (time $t+1$ oil price growth is higher in the shock series)

(iii) $u^{(S)}_{3,t+1} - u^{(B)}_{3,t+1} < 0$ (time $t+1$ world production growth is lower in the shock series)

If these sign restrictions are not fulfilled, generate new $u^{(B)}_{1,t+1}$ and $u^{(C)}_{1,t+1}$ and again check $(i) - (iii)$. For all $s > 1$, simulate $u^{(B)}_{t+s}$ and set $u^{(B)}_{t+s} = u^{(S)}_{t+s}$.

Step 3: For each state r, calculate the approximate conditional expectation of the time $t+1, ..., t+h$ benchmark and shock forecasts by averaging over all N values:

$$y^{(B)}_{r,t+s} = N^{-1} \sum_{n=1}^{N} y^{(B)}_{r,n,t+s}, \tag{B.5}$$

$$y^{(S)}_{r,t+s} = N^{-1} \sum_{n=1}^{N} y^{(S)}_{r,n,t+s}. \tag{B.6}$$

Step 4: Finally, for each state r calculate $\text{IRF}_{r,t} = (\text{IR}_{r,t+1}, ..., \text{IR}_{r,t+h})$ where

$$\text{IR}_{r,t+s} = y_{r,t+s}^{(S)} - y_{r,t+s}^{(B)}. \tag{B.7}$$

We follow Baumeister and Peersman (2013a) and set $R = 500$, $N = 100$ and $h = 26$, i.e. at each t, we simulate 500 possible states of the economy, each with a oil supply shock in $t+1$ and impulse responses up to 25 quarters after the shock.[16] As an illustration, Figure B1 plots these 500 IRFs obtained for 2010-Q1. Note that $t_b = t+1$ such that $t - t_b = 0$ is the time of the shock and $t - t_b > 0$ is the post-shock period.

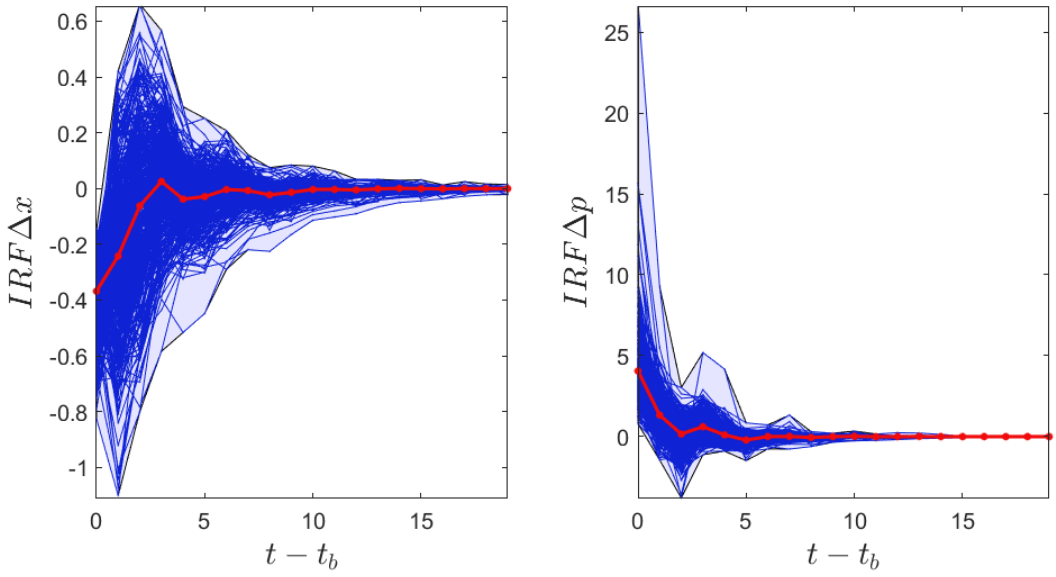

Figure B1: Simulated IRFs for 2010-Q1 (blue lines). t_b is the time of the supply shock, i.e. 2010-Q2. The red line is the average over all 500 IRFs.

[16] To estimate IRFs, we use the data set and the Matlab code provided by Baumeister and Peersman (2013a). Both is available at the Journal of Applied Econometrics data archive. Please note that we slightly adjusted the Matlab code to exclude any elasticity restrictions. For more details regarding these restrictions see Baumeister and Peersman (2013b). We also only consider the period 1972-Q1 to 2010-Q4. The original data set ranges from 1947-Q1 to 2010-Q4.

B.2 IRF based model parameter estimation

Our strategy is to use the simulated impulse responses to first estimate parameter ϕ which measures the sensitivity of the margin with respect to supply shortages. Then, we use the impulse responses to estimate the decay rate $\tilde{\kappa}$ in Equations (11) and (12). With values for ϕ and $\tilde{\kappa}$ we then obtain ψ via

$$\psi = \frac{\tilde{\kappa}}{\phi} \tag{B.8}$$

B.2.1 Model parameter ϕ

The first and second entries of the time t impulse responses for $t+s$ at state r, $\mathrm{IR}_{r,t+s}$, are

$$\mathrm{IR}_{1,r,t+s} = \delta x^{(S)}_{r,t+s} - \delta x^{(B)}_{r,t+s}, \tag{B.9}$$

$$\mathrm{IR}_{2,r,t+s} = \delta p^{(S)}_{r,t+s} - \delta p^{(B)}_{r,t+s}, \tag{B.10}$$

By construction, $\delta x^{(S)}_{r,t+s}$ and $\delta x^{(B)}_{r,t+s}$ are the expected oil supply growth rates with and without a negative oil supply shock in $t+1$, respectively (see Equations (B.4) and (B.3)). We can thus interpret $\mathrm{IR}_{1,r,t+s}$ as the expected time $t+s$ shortage in supply growth relative to the benchmark as caused by the supply shock. This supply shortage is mirrored in an expected excess price growth $\mathrm{IR}_{2,r,t+s}$. We use this relationship between $\mathrm{IR}_{1,r,t+s}$ and $\mathrm{IR}_{2,r,t+s}$ as a proxy for the relationship between supply shortage and price deviation as defined in Equation (8), i.e. $\Delta m_t = -\phi \Delta x_t$. This relationship is obtained via the econometric model

$$\mathrm{IR}_{2,r,t+s} = \alpha + \beta \mathrm{IR}_{1,r,t+s} + e_t. \tag{B.11}$$

The estimation results are provided in Table B1. The estimators provided in the second column are based on time t =1990-Q1, ...,2010-Q4 impulse responses, each with a forecast horizon of $s = 1, ..., 8$ for $r = 1, ..., 500$ different states of the economy, i.e. 320.000 simulated $\mathrm{IR}_1 \times \mathrm{IR}_2$ combinations. Although both estimators, $\hat{\alpha}$ and $\hat{\beta}$, are statistically significant, we can safely neglect $\hat{\alpha}$ due to its economic insignificance. Regarding our model Equation (8), the econometric model thus yields the relationship $m_t \approx -3\Delta x_t$, i.e. a supply shortage of 1 percent triggers a price increase of approximately 3 percent. This relationship is also illustrated in Figure B2.

	Sample Period		
	1990 - 2010	1990 - 1999	2000 - 2010
Parameter			
$\hat{\alpha}$	0.589	0.474	0.696
$\hat{\beta}$	-3.061	-3.720	-2.252

Table B1: OLS estimators of parameters α and β in Equation B.11. All p-values < 0.01.

To examine possible changes in the relationship between prices and supply within the 1990-2010 period, columns 3 and 4 of Table B1 provide estimates based on the time windows t =1990-Q1, ...,1999-Q4 and t =2000-Q1, ...,2010-Q4. Both samples thus encompass 160.000 simulated $\text{IR}_1 \times \text{IR}_2$ combinations. As can be seen, the constant $\hat{\alpha}$ is still economically insignificant. More interesting is the sensitivity of the oil price with respect to oil supply, which appears to be weaker for the 2000s compared to the 1990s. We account for this variation in the sensitivity by setting $\phi = 3$ in the base scenario, $\phi = 1.5$ in the optimistic scenario and $\phi = 4.5$ in the pessimistic scenario.

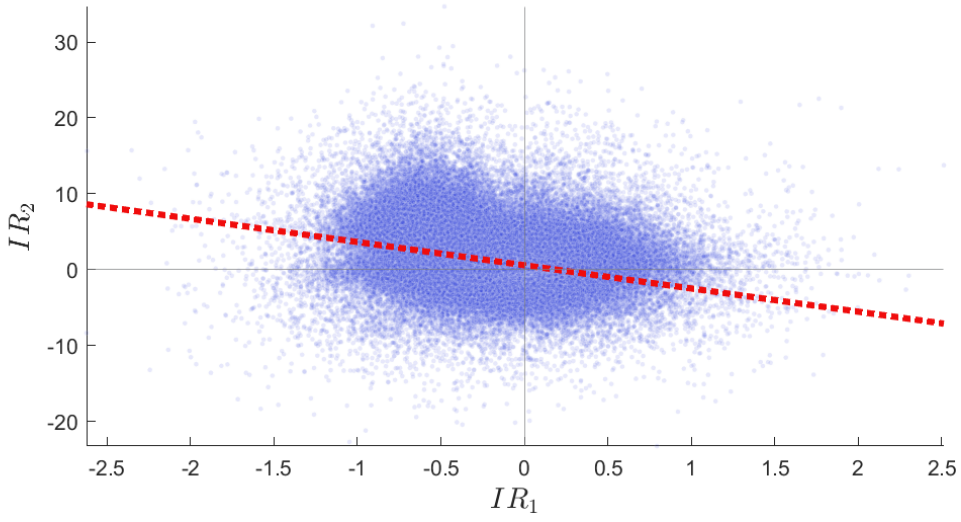

Figure B2: Impulse responses (blue dots) and estimated linear relationship (red line). The x-axis shows IR_1, interpreted as a supply shortage Δx_t, while the y-axis shows IR_2, interpreted as margin m_t. The graph shows a total of 320.000 simulated data points.

B.2.2 Decay rate $\tilde{\kappa}$

The adjustment processes are defined in Equations (11) and (12) as $\Delta x_t = \Delta x_{t_b}(1-\tilde{\kappa})^{(t-t_b)}$ and $m_t = m_{t_b}(1-\tilde{\kappa})^{(t-t_b)}$ where t_b is the time of the shock. We therefore rely on the impulse response functions IR_1 and IR_2 to serve as approximations to our decay processes. Because the simulated shock is $t+1$, we define the following econometric model for $i = 1, 2$:

$$\text{IR}_{i,r,t+s} = c_0(1-\tilde{\kappa})^{s-1} + e_t \tag{B.12}$$

where $s = 1, ..., 8$. Figure B1 indicates that impulse response functions may temporarily overshoot or undershoot. For this reason, we also define this model for capped IRs

$$\widetilde{\text{IR}}_{1,r,t+s} = \min(\text{IR}_{1,r,t+s}, 0), \tag{B.13}$$

$$\widetilde{\text{IR}}_{2,r,t+s} = \max(\text{IR}_{1,r,t+s}, 0). \tag{B.14}$$

The estimators of $\tilde{\kappa}$ based on the 1990 - 2000 sample period are shown in the second and third columns of Table B2. Due to over- and undershooting, non-capped IRs imply a faster adjustment than non-capped IRs. Nevertheless, all parameters suggest a reasonable full adjustment within 2 to 6 quarters (see Figure B2).

	Sample Period					
	1990 - 2000		1990 - 1999		2000 - 2010	
	Uncapped	Capped	Uncapped	Capped	Uncapped	Capped
Dependent variable: IR_1 and $\widetilde{\text{IR}}_1$						
$\hat{c}_0$	-0.554	-0.498	-0.609	-0.548	-0.498	-0.448
$\hat{\tilde{\kappa}}$	0.854	0.368	0.838	0.369	0.870	0.367
Dependent variable: IR_2 and $\widetilde{\text{IR}}_2$						
$\hat{c}_0$	5.689	5.619	5.932	5.863	5.446	5.386
$\hat{\tilde{\kappa}}$	0.741	0.536	0.752	0.575	0.730	0.498

Table B2: NLS estimators of parameters c_0 and $\tilde{\kappa}$. All p-values < 0.01.

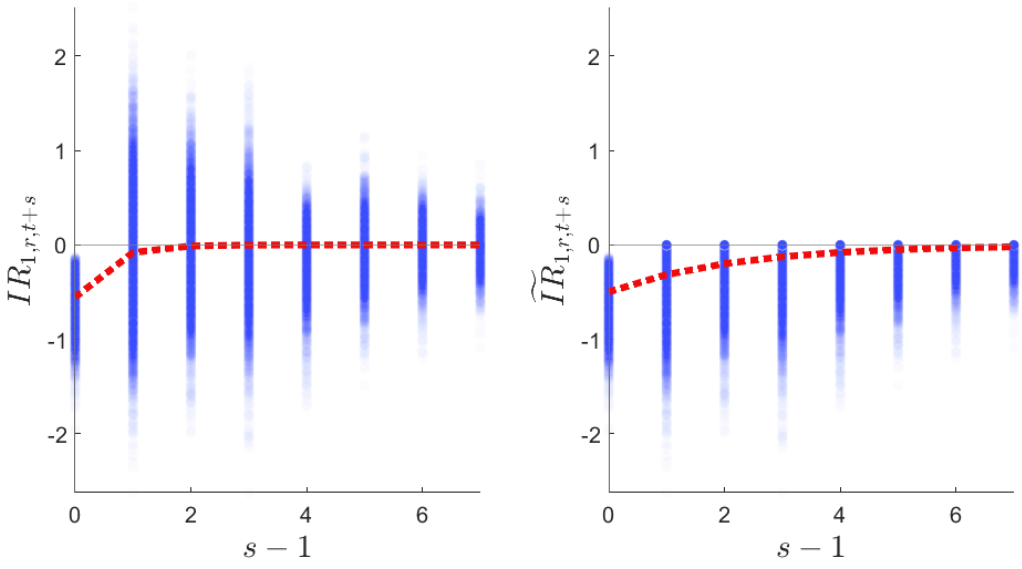

(**A**) Oil supply adjustment

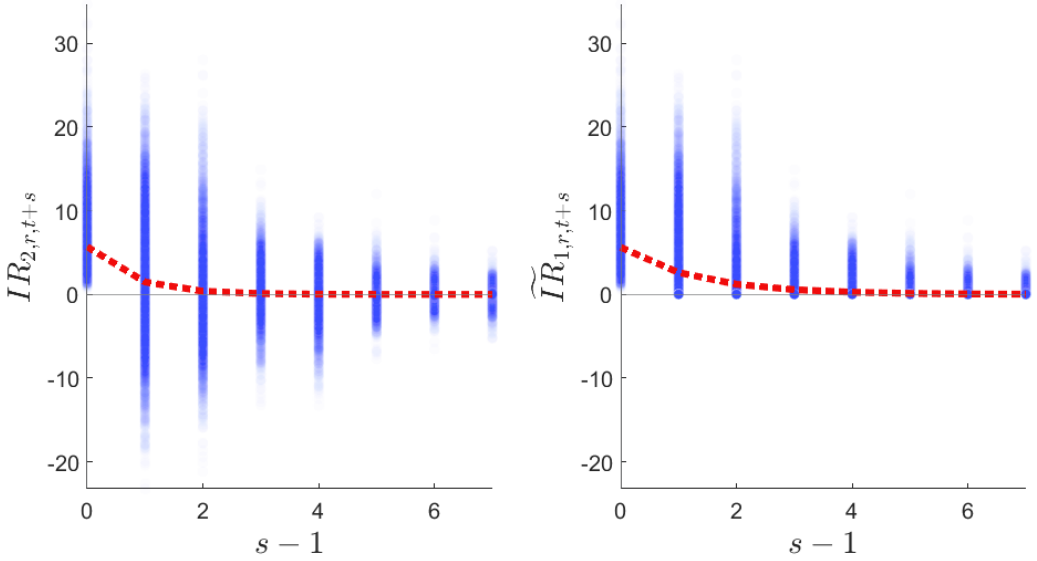

(**B**) Oil price adjustment

Figure B3: Impulse responses (blue dots) and estimated non-linear relationship (red dotted line.) The x-axis shows the time distance to the supply shock in $t+1$. The y-axis shows impulse responses of oil supply in panel A and oil prices in panel B. The estimated relationship is based on Equation (B.12) with parameters provided in column 2 and column 3 of Table B2.

Again, we also examine possible changes within the 1990-2000 period. Columns 4-7 of Table B2 provide estimators based on time t =1990-Q1, ...,1999-Q4 and time t =2000-Q1, ...,2010-Q4 impulse responses, respectively. Apparently, the dynamics are identical for these subperiods.

In summary, we decide to set $\tilde{\kappa} = 0.6$ in the base scenario, $\tilde{\kappa} = 0.3$ in the optimistic scenario and $\tilde{\kappa} = 0.9$ in the pessimistic scenario. These values for $\tilde{\kappa}$ cover the full range of the estimators provided in Table B2.

B.2.3 Model parameter ψ

The values we have set for the base scenario are $\phi = 3$ and $\tilde{\kappa} = 0.6$. The parameter ψ, which measures the speed of the supply adjustment over time is estimated from Equation (B.8) as $\psi = 0.2$. The $\phi \times \psi$ combinations for all scenarios are summarized in the following Table B3.

	Scenario		
	Base	Optimistic	Pessimistic
Parameter			
ϕ	3.000	1.500	4.500
$\tilde{\kappa}$	0.600	0.900	0.300
ψ	0.200	0.600	0.070

Table B3: Values for ϕ, $\tilde{\kappa}$ and ψ in the base-, the optimistic- and the pessimistic scenario.

Appendix C Additional Figures and Tables

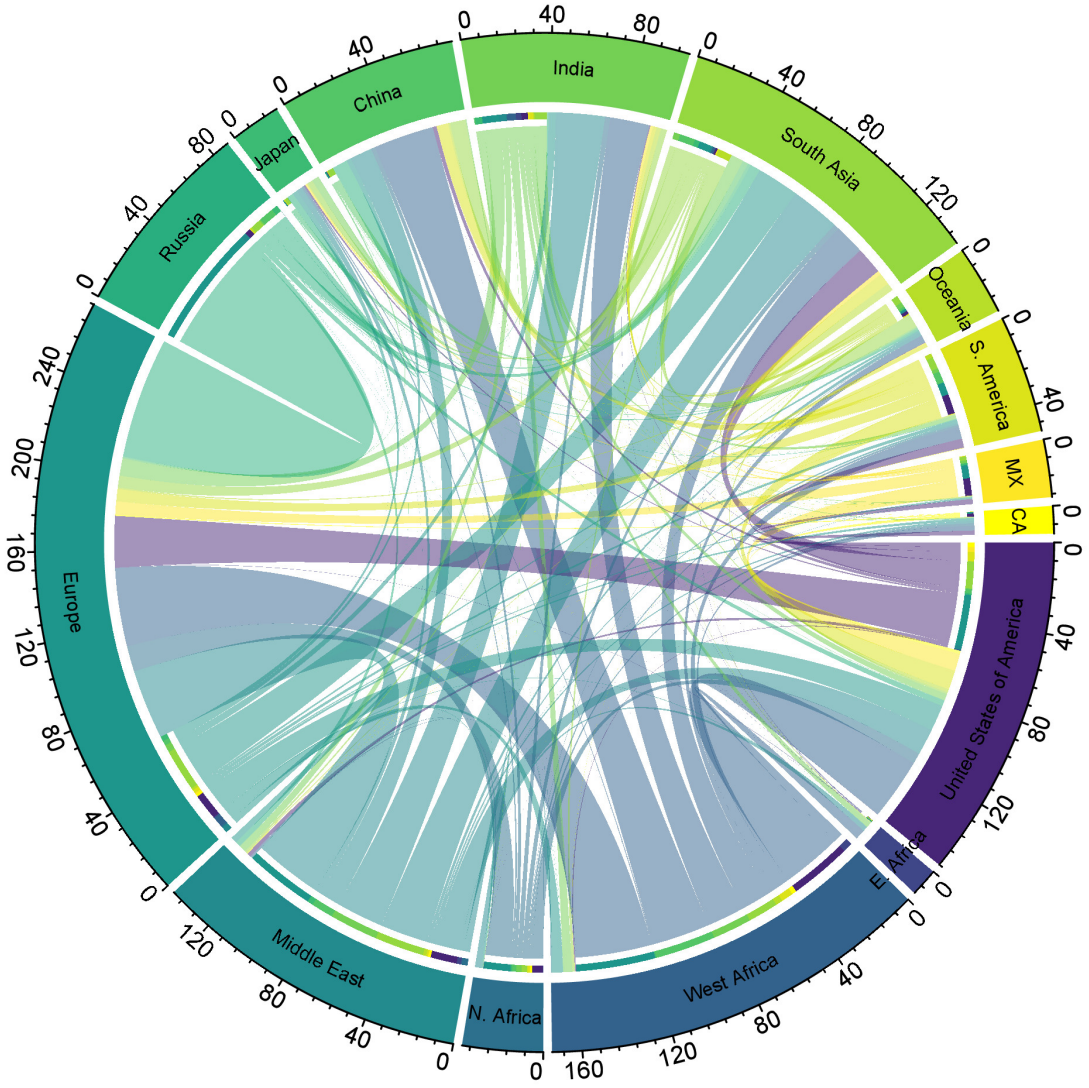

Figure C1: Empirical Network of Physical Oil Flows (2007 - 2018).
This figure shows average annual flows of crude oil and refined products in million barrels. the color coding visualizes the direction of the flows. For instance, the United states is importing significant amounts of crude oil products from West Africa, the Middle East, Europe, and Mexico, but exports to Europe and South Asia.

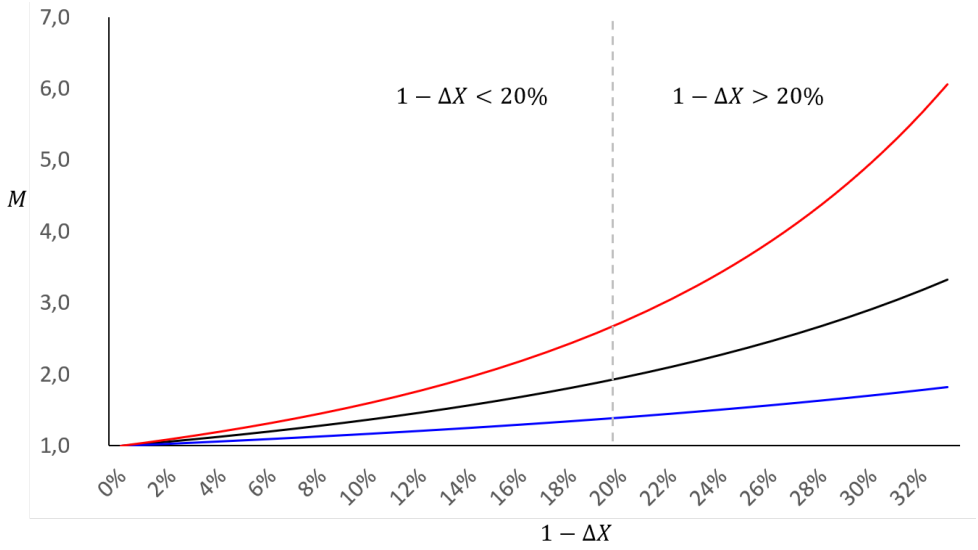

Figure C2: The x-axis of this Figure shows the relative supply shortage $1 - \Delta X$ while the y-axis shows the corresponding margin multiplier $M_t = (\Delta X)^{-\phi}$. The blue line shows M_t in case of $\phi = 1.5$ (optimistic scenario). The black line shows M_t in case of $\phi = 3.0$ (base scenario). The red line shows M_t in case of $\phi = 4.5$ (pessimistic scenario). Left of the vertical line, the supply shortage is below 20%.

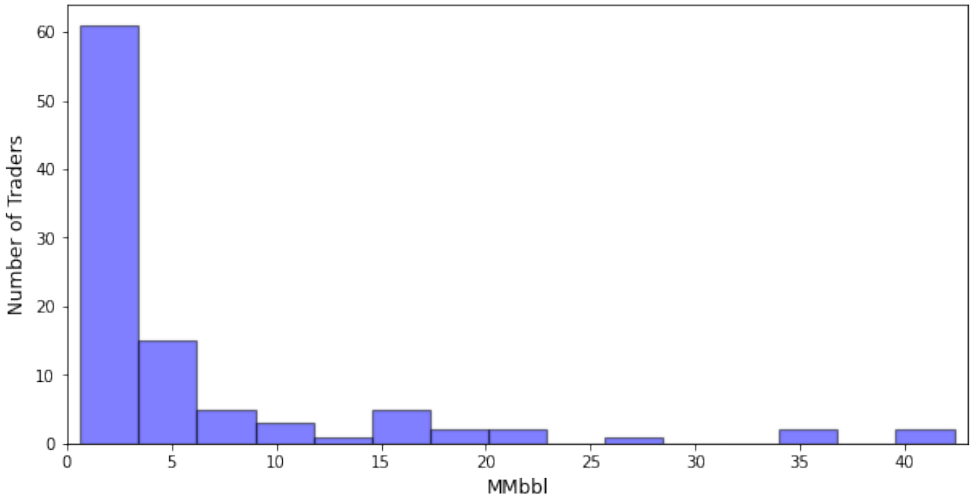

Figure C3: This figure shows the distribution of the empirical network among volumes in MMbbl across of the top 100 traders.

	Canada	Mexico	South America	USA	East Africa	North Africa	West Africa	Europe	Russia	Middle East	China	India	Japan	Oceania	South Asia	∑
Americas																
Canada	-	0.02	0.114	2.20	0.01	1.28	2.13	1.14	0.10	0.94	0.02	0.41	0.00	0.05	0.01	8.41
Mexico	0.00	-	0.075	2.67	0.01	0.00	0.02	0.75	0.00	0.18	0.10	0.32	0.02	0.16	0.18	4.47
South America	0.11	0.18	-	4.72	0.04	1.15	5.97	1.70	0.29	0.93	0.03	1.95	0.06	0.35	0.47	17.95
USA	1.33	9.01	9.87	-	0.15	5.40	32.33	11.87	2.43	13.43	0.21	3.12	0.03	1.67	0.97	91.81
EMEA																
East Africa	0.00	0.00	0.06	0.03	-	0.04	5.27	0.44	0.02	1.48	0.01	2.64	0.00	0.10	0.29	10.37
North Africa	0.00	0.00	0.00	0.03	0.00	-	0.03	0.85	0.09	2.59	0.00	0.19	0.00	0.00	0.02	3.81
West Africa	0.00	0.01	0.13	0.52	0.03	0.18	-	5.46	0.10	0.50	0.06	4.67	0.00	0.00	1.32	12.97
Europe	0.69	6.81	6.38	26.65	0.29	12.91	40.49	-	60.83	31.27	0.68	8.61	0.43	0.74	6.07	202.85
Russia	0.00	0.00	0.01	0.01	0.00	0.00	0.01	0.04	-	0.09	0.00	0.00	0.00	0.00	0.00	0.17
Middle East	0.06	0.13	0.11	2.00	0.06	0.59	0.51	3.13	2.58	-	0.04	3.39	0.09	0.50	0.98	14.15
APAC																
China	0.01	0.25	5.86	2.04	0.04	2.06	31.64	2.36	7.79	10.23	-	0.52	0.23	0.99	7.94	71.95
India	0.05	1.33	1.89	0.41	0.18	2.41	18.50	3.43	0.65	18.68	0.08	-	0.01	2.42	1.91	51.93
Japan	0.00	0.89	0.13	0.86	0.01	0.87	0.54	2.17	3.08	2.68	0.15	3.41	-	0.44	2.52	17.75
Oceania	0.02	0.33	2.08	0.15	0.06	0.26	3.68	1.12	0.77	1.45	0.35	0.58	0.60	-	6.49	17.93
South Asia	0.02	1.91	6.22	13.77	0.26	2.59	13.97	21.78	4.18	22.07	2.92	6.34	1.51	3.81	-	101.35
∑	2.29	20.85	32.93	56.04	1.13	29.74	155.10	56.24	82.90	106.53	4.64	36.13	2.97	11.24	29.15	627.86

Table D1: Aggregate Physical Oil Flows (2007 - 2018)

This Table shows aggregated annual oil flows from exporting regions labeled in the columns to destination regions labeled in the rows. For instance, the United States imported on average 9.01 million barrel of oil and refined oil products from Mexico on an annual basis. This table is constructed by aggregating across 155,435 individual vessel transactions from 2007 - 2018.

	UNIPEC	SHELL	BP	VITOL	CNR	PETROBRAS	CSSSA	REPSOL	CLEARLAKE	ST SHIPPING
Americas										
Canada	0.000	0.089	0.246	0.027	0.253	0.000	0.000	0.022	0.000	0.020
Mexico	0.440	2.387	0.175	0.110	0.446	0.021	0.018	5.676	0.017	0.032
South America	1.858	3.686	0.904	0.816	1.118	10.638	0.052	1.798	0.435	0.194
USA	1.846	4.191	3.333	4.372	4.806	0.461	2.285	1.220	1.813	2.581
EMEA										
East Africa	0.013	0.032	0.029	0.059	0.044	0.011	0.032	0.000	0.000	0.020
North Africa	1.783	1.453	2.235	0.513	0.304	0.793	1.225	1.776	0.197	0.579
West Africa	21.526	9.161	11.127	6.261	3.423	5.457	8.069	3.184	0.593	2.095
Europe	1.436	3.106	3.958	3.701	3.038	0.668	1.203	0.751	3.204	1.083
Russia	4.355	7.101	2.392	10.087	1.553	0.008	2.460	0.806	6.978	5.315
Middle East	6.499	4.403	4.961	3.777	2.305	0.628	2.753	3.742	1.389	2.022
APAC										
China	0.612	0.267	0.126	0.227	0.251	0.034	0.048	0.022	0.084	0.076
India	0.349	2.278	3.295	2.011	2.112	1.398	0.893	0.022	1.479	1.517
Japan	0.013	0.292	0.146	0.143	0.396	0.034	0.000	0.007	0.010	0.087
Oceania	0.200	0.469	0.627	0.220	0.341	0.131	0.646	0.391	0.081	0.133
South Asia	1.420	1.803	2.779	2.773	2.466	0.594	0.122	0.162	0.585	0.714
$\sum$	42.350	40.719	36.333	35.096	22.856	20.875	19.808	19.579	16.865	16.468

Table D2: Commodity Trader Default and Absolute Oil Exports (Uncapped)

This table shows the reduction in physical oil flows following the bankruptcy of a large commodity trader. It takes the perspective of an oil exporting region. Flow reductions are measured in million barrels for the quarter in which the shock occurs. For instance, the failure of the Chinese oil trader Unipec in the first column of the table is estimated to cause oil exports from West Africa to fall by 21 million barrel in the quarter of the shock.

	UNIPEC	SHELL	BP	VITOL	CNR	PETROBRAS	CSSSA	REPSOL	CLEARLAKE	ST SHIPPING
Americas										
Canada	0.000	0.426	0.522	0.351	0.155	0.006	0.012	0.011	0.054	0.050
Mexico	0.040	0.078	0.089	0.078	0.418	0.006	0.006	0.003	0.008	0.040
South America	0.082	0.812	0.649	0.571	0.873	8.032	0.065	1.054	0.147	0.280
USA	0.589	8.937	6.722	3.912	3.041	3.722	1.815	0.793	2.862	1.372
EMEA										
East Africa	0.007	1.065	1.605	0.338	0.215	0.006	0.373	0.046	0.056	0.191
North Africa	0.000	0.057	0.078	0.142	0.061	0.000	0.010	0.018	0.097	0.083
West Africa	0.072	0.200	0.974	1.129	1.372	0.012	0.202	0.009	0.379	0.590
Europe	3.636	15.429	10.784	15.708	6.899	1.864	13.080	16.379	7.666	8.467
Russia	0.000	0.000	0.032	0.009	0.019	0.000	0.002	0.000	0.000	0.004
Middle East	0.072	1.133	0.765	0.741	1.105	0.051	0.438	0.357	1.030	0.391
APAC										
China	33.887	1.541	0.658	1.406	1.198	2.712	0.234	0.087	0.456	0.757
India	0.025	0.427	5.396	0.174	0.207	0.666	0.137	0.019	0.166	0.244
Japan	0.338	1.142	0.677	0.996	1.095	0.347	0.476	0.321	0.598	0.480
Oceania	0.026	1.595	2.621	2.274	0.627	0.472	0.035	0.025	0.206	0.195
South Asia	3.575	7.876	4.761	7.266	5.571	2.979	2.922	0.458	3.140	3.324
$\sum$	42.350	40.719	36.333	35.096	22.856	20.875	19.808	19.579	16.865	16.468

Table D3: Commodity Trader Default and Absolute Oil Imports (Uncapped)

This table shows the reduction in physical oil flows following the bankruptcy of a large commodity trader. It takes the perspective of an oil importing region. Flow reductions are measured in million barrels for the quarter in which the shock occurs. For instance, the failure of the Chinese oil trader Unipec in the first column of the table is estimated to cause import reductions in China of more than 33 million barrel in the quarter of the shock.

	UNIPEC	SHELL	BP	VITOL	CNR	PETROBRAS	CSSSA	REPSOL	CLEARLAKE	ST SHIPPING
Americas										
Canada	0.000	0.089	0.246	0.027	0.253	0.000	0.000	0.022	0.000	0.020
Mexico	**0.311**	2.387	0.175	0.110	0.446	**0.019**	0.018	5.676	0.017	0.032
South America	**1.298**	3.686	0.904	0.816	1.118	10.638	0.052	1.798	0.435	0.194
USA	**1.306**	4.191	3.333	4.372	4.806	**0.233**	2.285	1.220	1.813	2.581
EMEA										
East Africa	**0.009**	0.032	0.029	0.059	0.044	**0.005**	0.032	0.000	0.000	0.020
North Africa	**0.977**	1.453	2.235	0.513	0.304	**0.397**	1.225	1.776	0.197	0.579
West Africa	**9.556**	9.161	11.127	6.261	3.423	**3.088**	8.069	3.184	0.593	2.095
Europe	**0.895**	3.106	3.958	3.701	3.038	**0.441**	1.203	0.751	3.204	1.083
Russia	**2.992**	7.101	2.392	10.087	1.552	**0.008**	2.460	0.806	6.978	5.315
Middle East	**3.772**	4.403	4.961	3.777	2.305	**0.313**	2.753	3.742	1.389	2.022
APAC										
China	0.612	0.267	0.126	0.227	0.251	**0.028**	0.048	0.022	0.084	0.076
India	**0.347**	2.278	3.295	2.011	2.112	**0.714**	0.893	0.022	1.479	1.517
Japan	**0.010**	0.292	0.146	0.143	0.396	**0.029**	0.000	0.007	0.010	0.087
Oceania	**0.092**	0.469	0.627	0.220	0.341	**0.099**	0.646	0.391	0.081	0.133
South Asia	**0.678**	1.803	2.779	2.773	2.466	**0.421**	0.122	0.162	0.585	0.714
$\sum$	**22.853**	40.719	36.333	35.096	22.856	**16.433**	19.808	19.579	16.865	16.468

Table D4: Commodity Trader Default and Absolute Oil Exports (Capped)

This Table shows the reduction in oil flows from the perspective of an exporting region. Flow reductions are measured in million barrels for the quarter in which the shock occurs. Bold numbers indicate adjusted contributions, such that supply reductions caused by a trader's default do not exceed 20%. For instance, the failure of Petrobras in the 6$^{\text{th}}$ column temporarily reduces oil exports from South America by more than 10 million barrels.

	UNIPEC	SHELL	BP	VITOL	CNR	PETROBRAS	CSSSA	REPSOL	CLEARLAKE	ST SHIPPING
Americas										
Canada	0.000	0.426	0.522	0.351	0.155	0.006	0.012	0.011	0.054	0.050
Mexico	0.040	0.078	0.089	0.078	0.418	0.006	0.006	0.003	0.008	0.040
South America	0.082	0.812	0.649	0.571	0.873	**3.590**	0.065	1.054	0.147	0.280
USA	0.589	8.937	6.722	3.912	3.041	3.722	1.815	0.793	2.862	1.372
EMEA										
East Africa	0.007	1.065	1.605	0.338	0.215	0.006	0.373	0.046	0.056	0.191
North Africa	0.000	0.057	0.077	0.142	0.061	0.000	0.010	0.018	0.097	0.083
West Africa	0.072	0.200	0.974	1.129	1.372	0.012	0.202	0.009	0.379	0.590
Europe	3.636	15.429	10.784	15.708	6.899	1.864	13.080	16.379	7.666	8.467
Russia	0.000	0.000	0.033	0.009	0.019	0.000	0.002	0.000	0.000	0.004
Middle East	0.072	1.133	0.765	0.741	1.105	0.051	0.438	0.357	1.030	0.391
APAC										
China	**14.390**	1.541	0.658	1.406	1.198	2.712	0.234	0.087	0.456	0.757
India	0.025	0.427	5.396	0.174	0.207	0.666	0.137	0.019	0.166	0.243
Japan	0.338	1.142	0.677	0.996	1.095	0.347	0.476	0.321	0.598	0.480
Oceania	0.026	1.595	2.621	2.274	0.627	0.472	0.035	0.025	0.206	0.195
South Asia	3.575	7.876	4.761	7.266	5.571	2.979	2.922	0.458	3.140	3.324
$\sum$	22.853	40.719	36.333	35.096	22.856	16.433	19.808	19.579	16.865	16.468

Table D5: Commodity Trader Default and Absolute Oil Imports (Capped)

This table shows the reduction in physical oil flows following the bankruptcy of a large commodity trader. It takes the perspective of an oil importing region. Flow reductions are measured in million barrels for the quarter in which the shock occurs. Bold numbers indicate adjusted contributions, such that supply reductions caused by a trader's default do not exceed 20%. For instance, the failure of the Chinese oil trader Unipec in the first column of the table is estimated to cause import reductions in China of more than 14.39 million barrel in the quarter of the shock and is therefore capped at 14.39.

	Mexico	South America	USA	East Africa	North Africa	West Africa	Europe	Russia	Middle East	China	India	Japan	Oceania	South Asia
Americas														
Canada	0.760	0.738	0.753	1.204	0.743	0.962	0.730	0.807	1.101	1.407	1.139	1.358	1.344	1.327
Mexico		0.620	0.538	1.254	0.865	0.975	0.936	1.044	1.228	1.275	1.266	1.225	1.212	1.402
South America			0.621	1.204	0.994	0.882	0.823	1.192	1.170	1.229	0.990	1.131	1.156	1.500
USA				1.248	0.857	0.918	0.776	1.001	1.093	1.276	1.258	1.226	1.213	1.394
EMEA														
East Africa					0.915	0.862	1.130	0.868	0.623	1.091	0.702	1.011	1.031	0.806
North Africa						0.837	0.576	0.668	0.802	1.232	0.826	1.250	1.302	0.900
West Africa							0.845	0.839	0.742	1.284	1.012	1.353	1.219	1.179
Europe								0.660	0.997	1.178	1.020	1.348	1.398	1.185
Russia									0.824	1.464	0.934	0.834	1.124	0.803
Middle East										0.946	0.691	0.988	0.721	0.770
APAC														
China											0.895	0.563	0.831	0.677
India												0.836	0.914	0.654
Japan													0.828	0.707
Oceania														0.833

Table D6: This table shows the matrix of region specific distance measures D_{ij}. First, kilometer distance data for tanker routes was obtained from the Worldscale database and complemented with data from Searoutes.com. Second, the kilometer distance was standardized between 0.5 and 1.5 with values of 1 indicating average distances (around 15,000 km). For instance, the distance between the ports of Itaqui in Brazil and Onsan in South Korea is 24,507 km by ship. This distance translates to an effective 50% markup over prices. The shortest distance in our data is between the ports of Altamira in Mexico and Houston in the United States (928 km).